

Heterometallic titanium-gold complexes inhibit renal cancer cells *in vitro* and *in vivo*.

Jacob Fernández-Gallardo,^{†a} Benelita T. Elie,^{†a,b} Tanmoy Sadhukha,^c Swayam Prabha,^{c,d} Mercedes Sanaú,^e Susan A. Rotenberg,^{b,f} Joe W. Ramos,^{*g} and María Contel^{*a,b,g}

Supplementary Information

Table of Contents

1. NMR spectra of compounds 5 , 6 and 7 in CDCl ₃	2
2. Selected NMR spectra of decomposition of compounds 5 and 7 in DMSO-d ₆	7
3. UV-visible spectra of compound 4 , 5 , 6 and 7 in different solvents.....	10
4. Selected UV-visible spectra of decomposition of compounds 5 and 7 in 1:99 DMSO/PBS-1X.....	15
5. Solid state IR spectra of compounds 4 , 5 , 6 and 7	16
6. ESI+ mass spectra of compounds 5 and 7 and theoretical isotopic distributions of relevant peaks ...	18
7. Crystallographic data for compound 6	20
8. DFT Studies for compounds 4 , 5 , 6 and 7	22
8.1. Comparison of Selected Geometrical Properties	22
8.2. Optimized geometries and cartesian coordinates of stationary points	24
8.3. Calculated IR spectra of compounds 4 , 5 , 6 and 7	28
9. Cytotoxicity Assays (IC ₅₀ values after 24 and 72 hours of treatment).....	31
10. Migration assays with compounds 3 and 5	32
11. Inhibition of Thioredoxin Reductase (TrxR) studies of compounds 3 , 5 and Auranofin at 5, 12 and 24 h.	33
12. Inhibition studies of a panel of 35 protein kinases of oncological interest of compound 5	34
13. Effects of Auranofin on MAPKAPK-3 in Caki-1 cells	36
14. Effect of compound 3 on Caki-1 mouse xenografts	37

1. NMR spectra of compounds **5**, **6** and **7** in CDCl_3

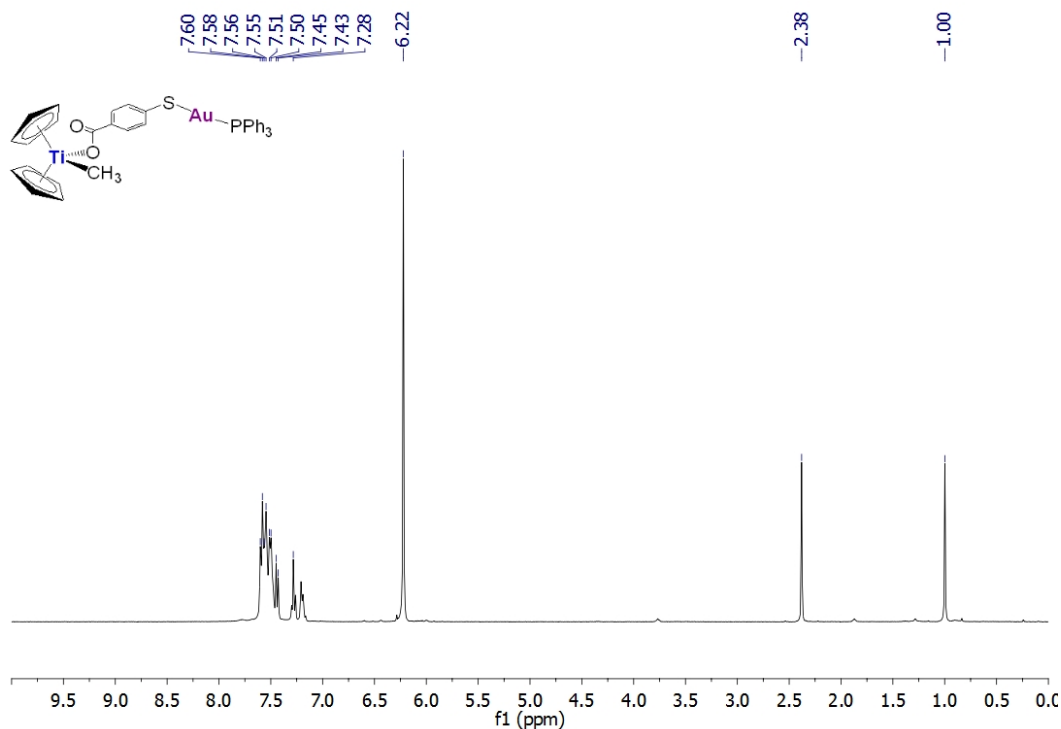


Figure S1. ^1H NMR spectrum of compound **5** in CDCl_3 .

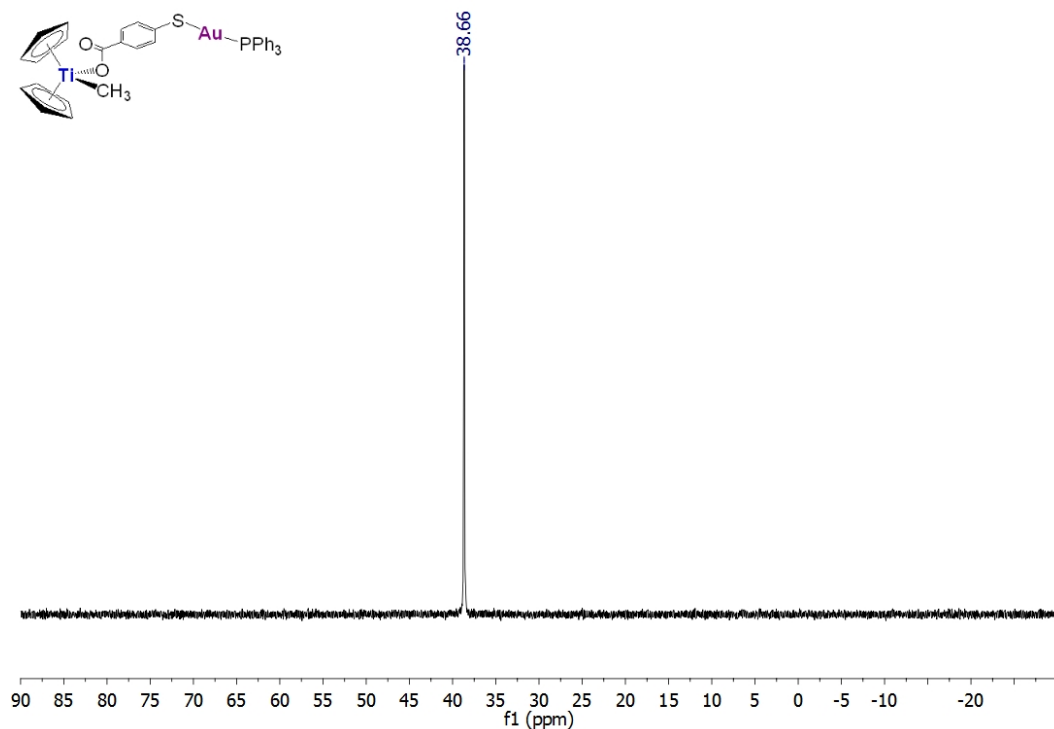


Figure S2. $^{31}\text{P}\{^1\text{H}\}$ NMR spectrum of compound **5** in CDCl_3 .

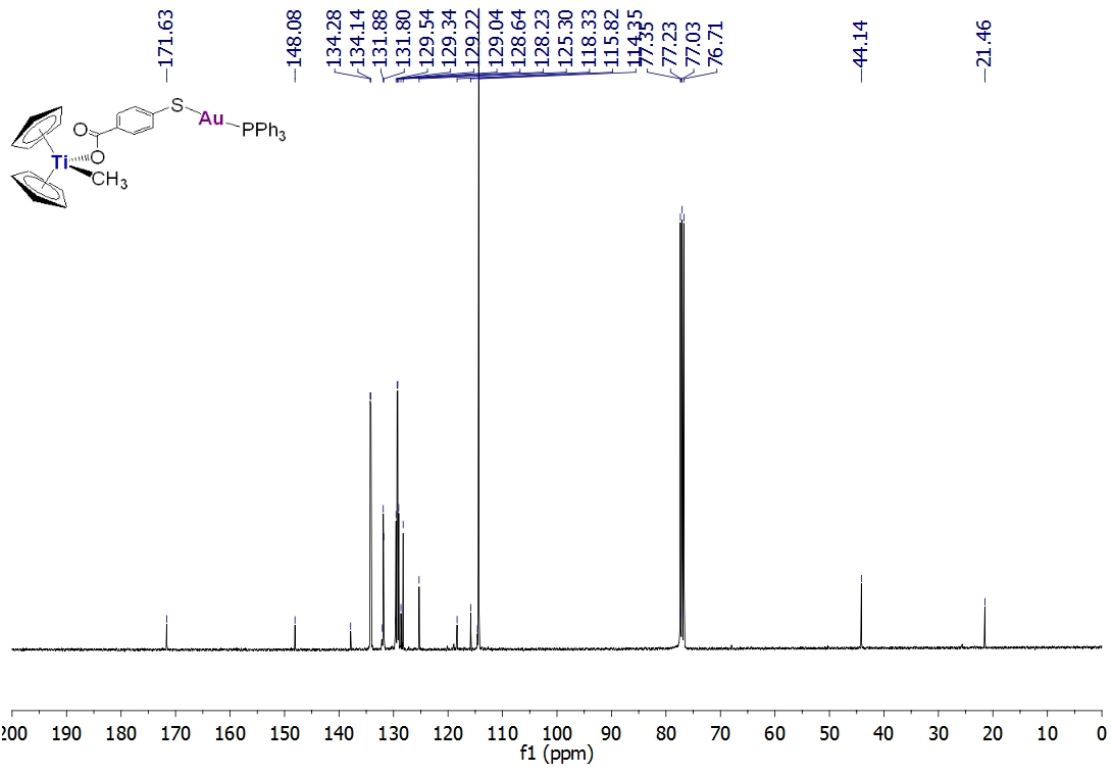


Figure S3. $^{13}\text{C}\{\text{H}\}$ NMR spectrum of compound **5** in CDCl_3 .

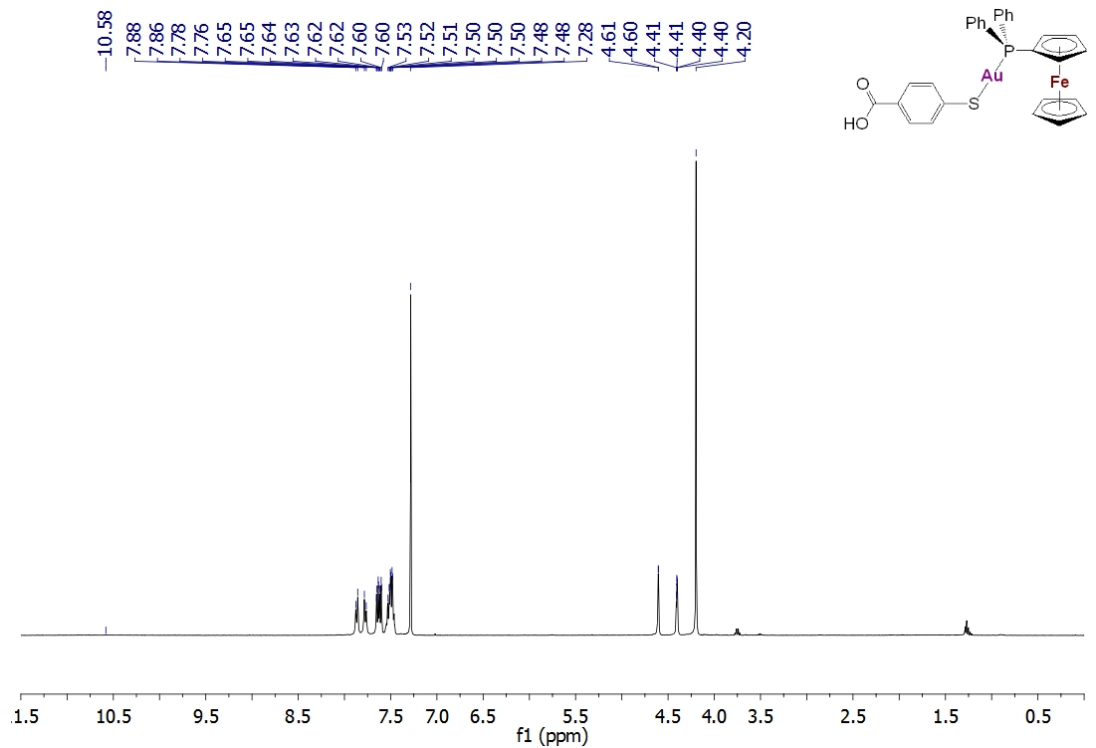


Figure S4. ^1H NMR spectrum of compound **6** in CDCl_3 .

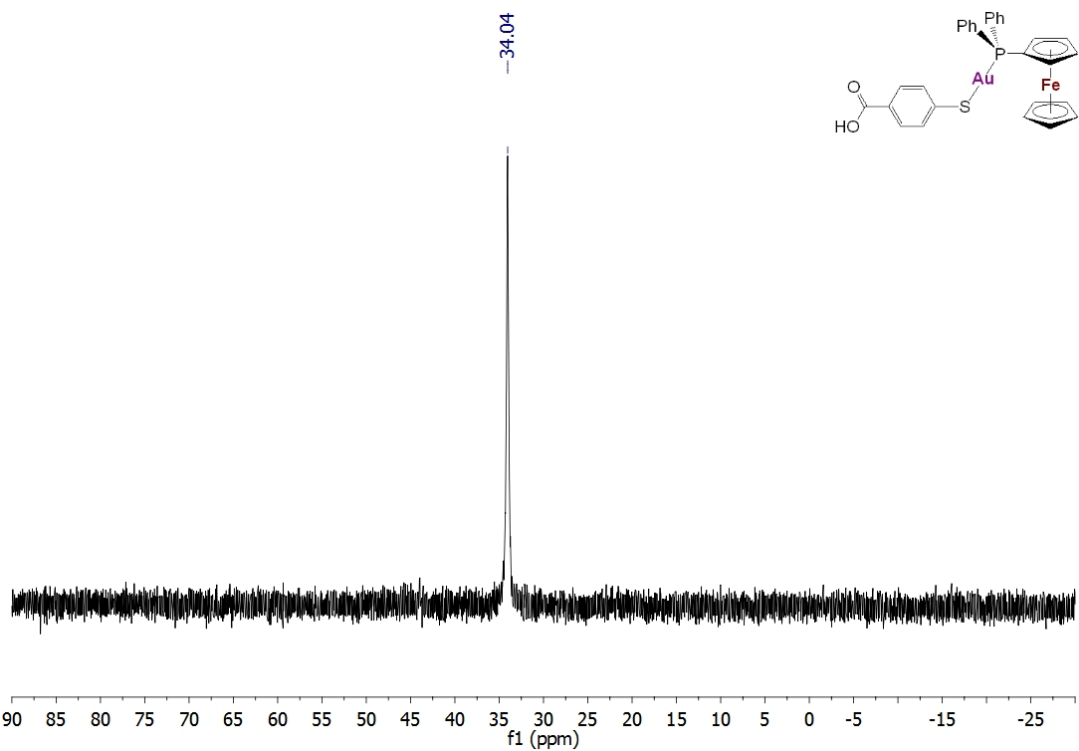


Figure S5. $^{31}\text{P}\{\text{H}\}$ NMR spectrum of compound **6** in CDCl_3 .

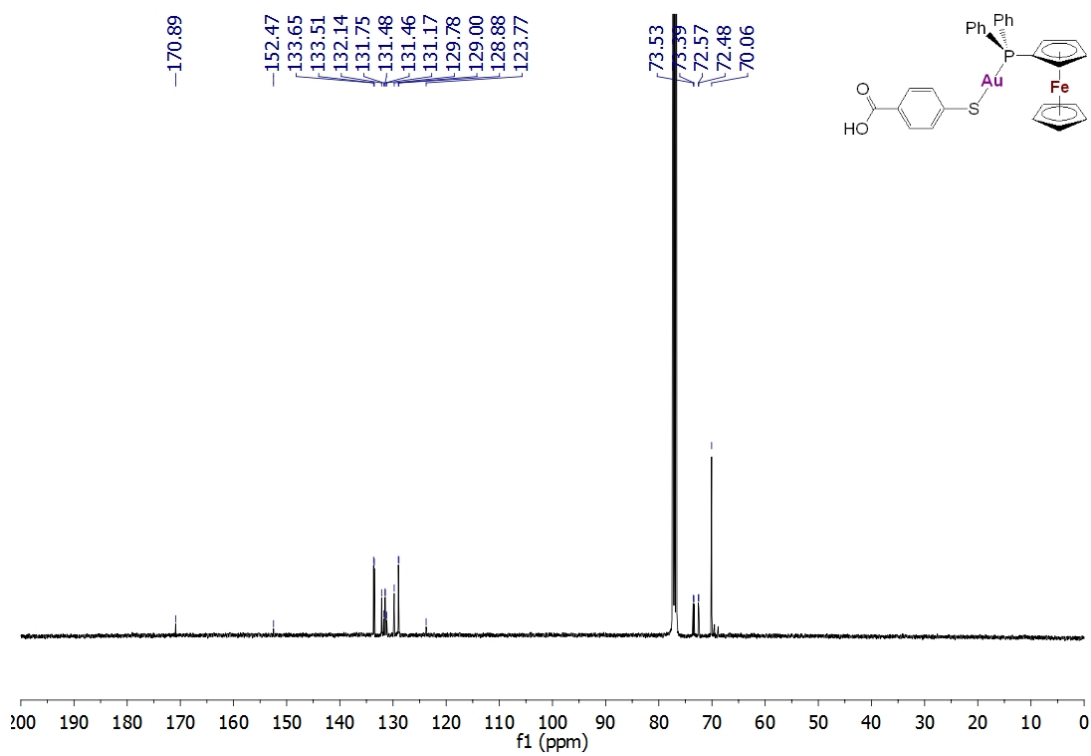


Figure S6. $^{13}\text{C}\{\text{H}\}$ NMR spectrum of compound **6** in CDCl_3 .

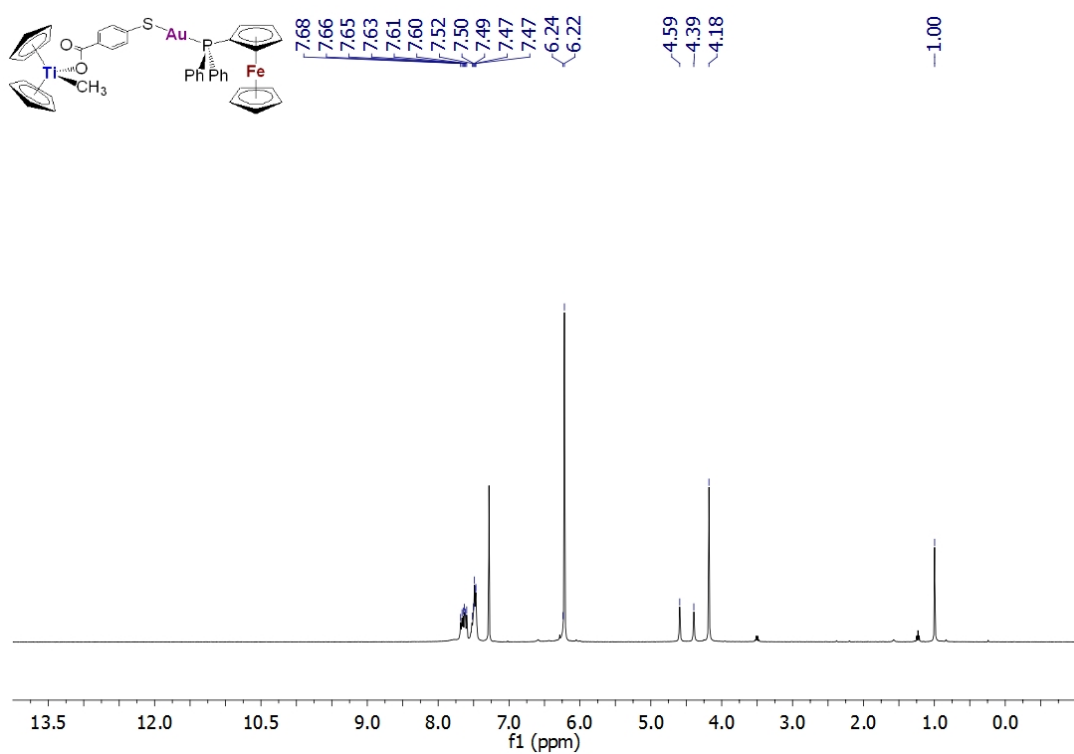


Figure S7. ^1H NMR spectrum of compound **7** in CDCl_3 .

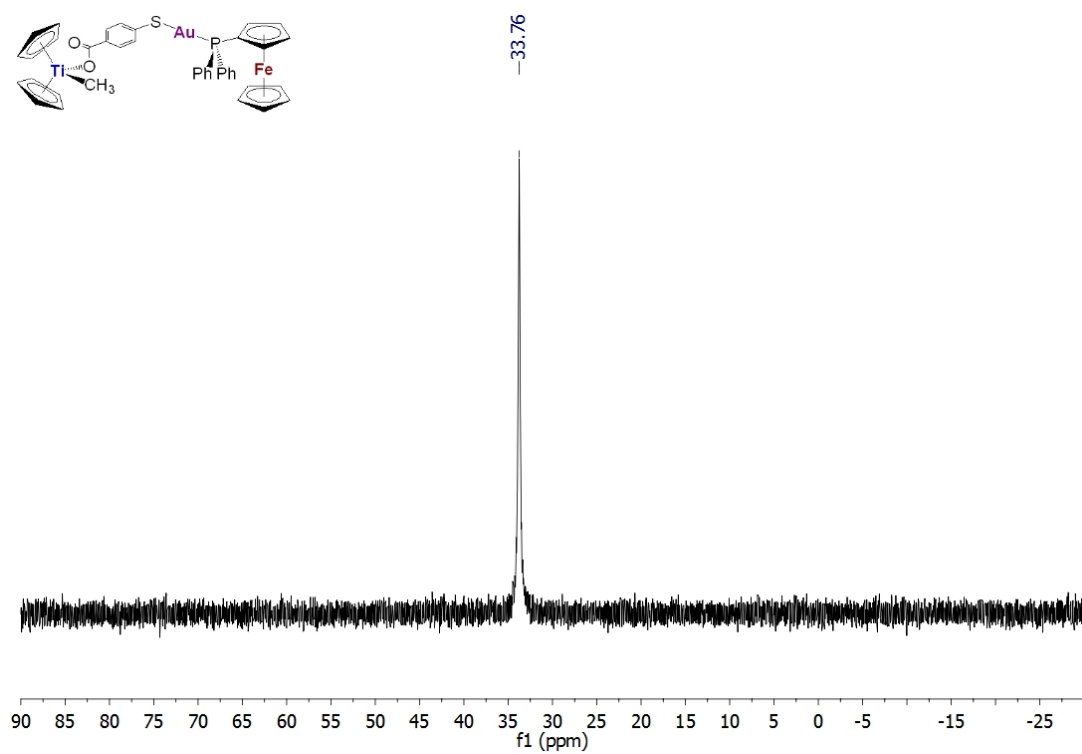


Figure S8. $^{31}\text{P}\{^1\text{H}\}$ NMR spectrum of compound **7** in CDCl_3 .

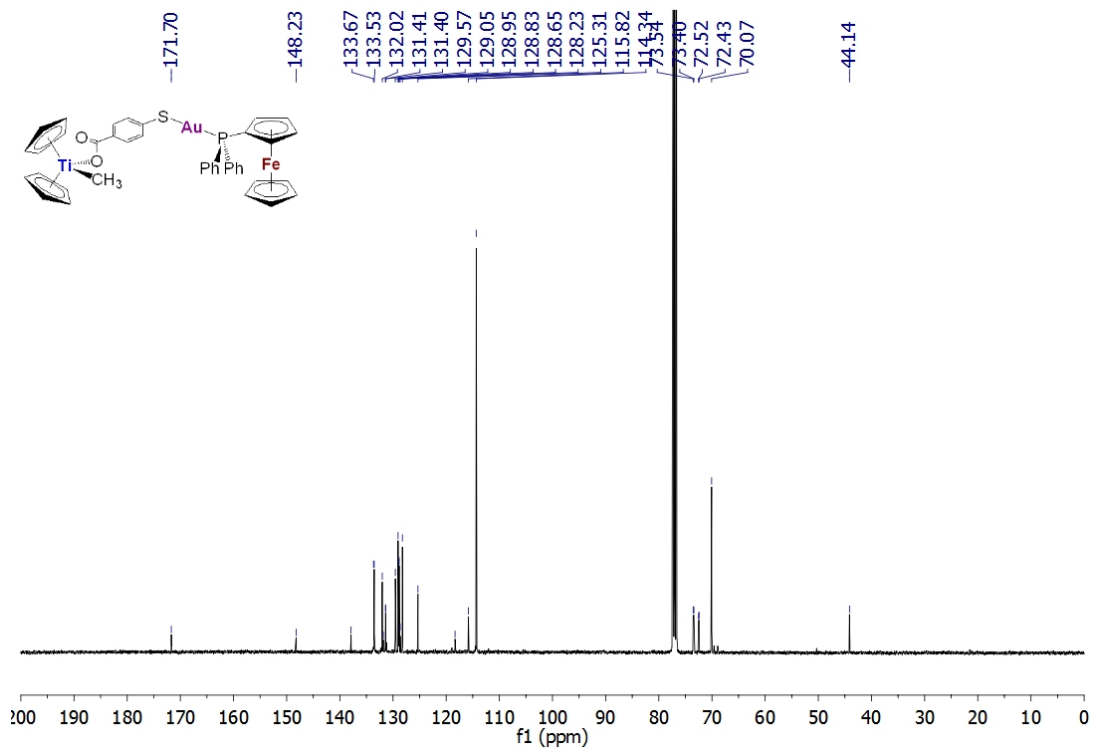


Figure S9. $^{13}\text{C}\{^1\text{H}\}$ NMR spectrum of compound 7 in CDCl_3 .

2. Selected NMR spectra of decomposition of compounds **5 and **7** in DMSO-*d*₆**

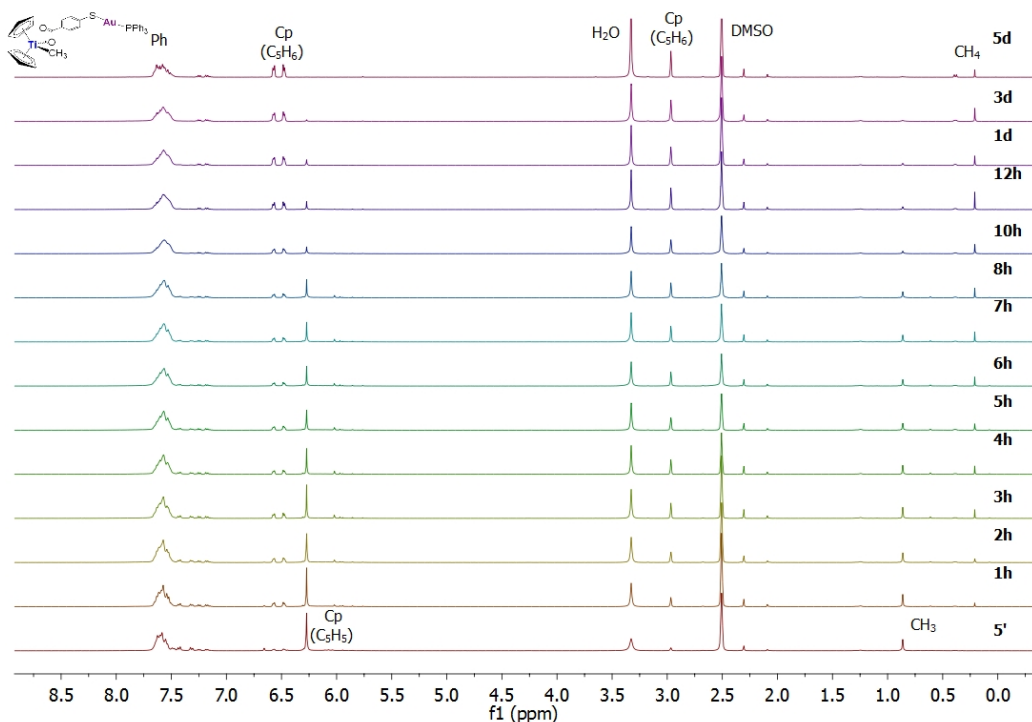


Figure S10. ¹H NMR spectrum in DMSO-*d*₆. Decomposition of compound **5** over time. t_½=8h.

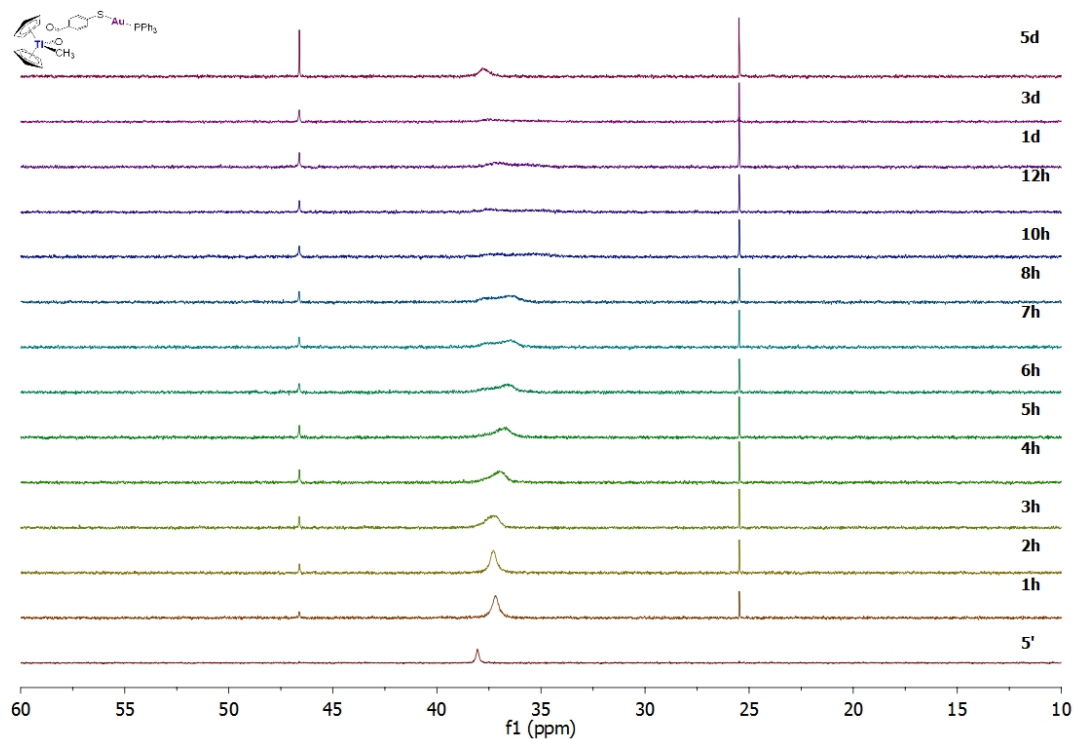


Figure S11. ³¹P{¹H} NMR spectrum in DMSO-*d*₆. Decomposition of compound **5** over time. t_½=8h.

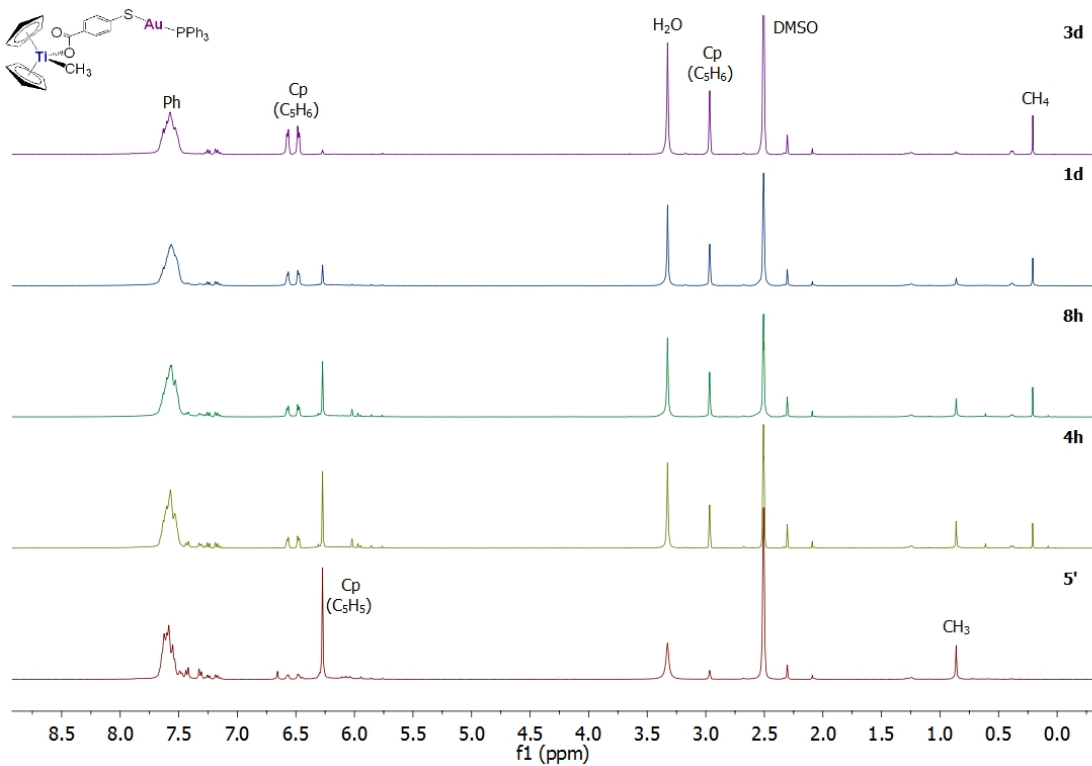


Figure S12. ¹H NMR spectrum in DMSO-*d*₆. Decomposition of compound **5** over time. *t*_½=8h.

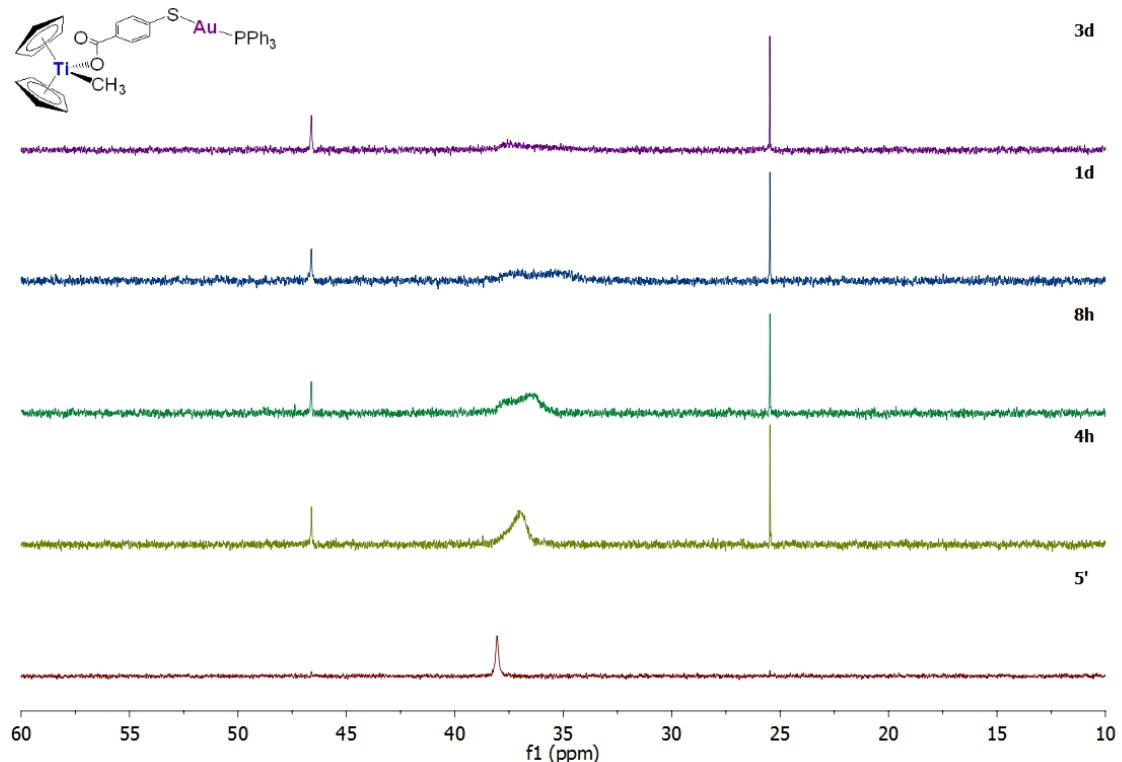


Figure S13. ³¹P{¹H} NMR spectrum in DMSO-*d*₆. Decomposition of compound **5** over time. *t*_½=8h.

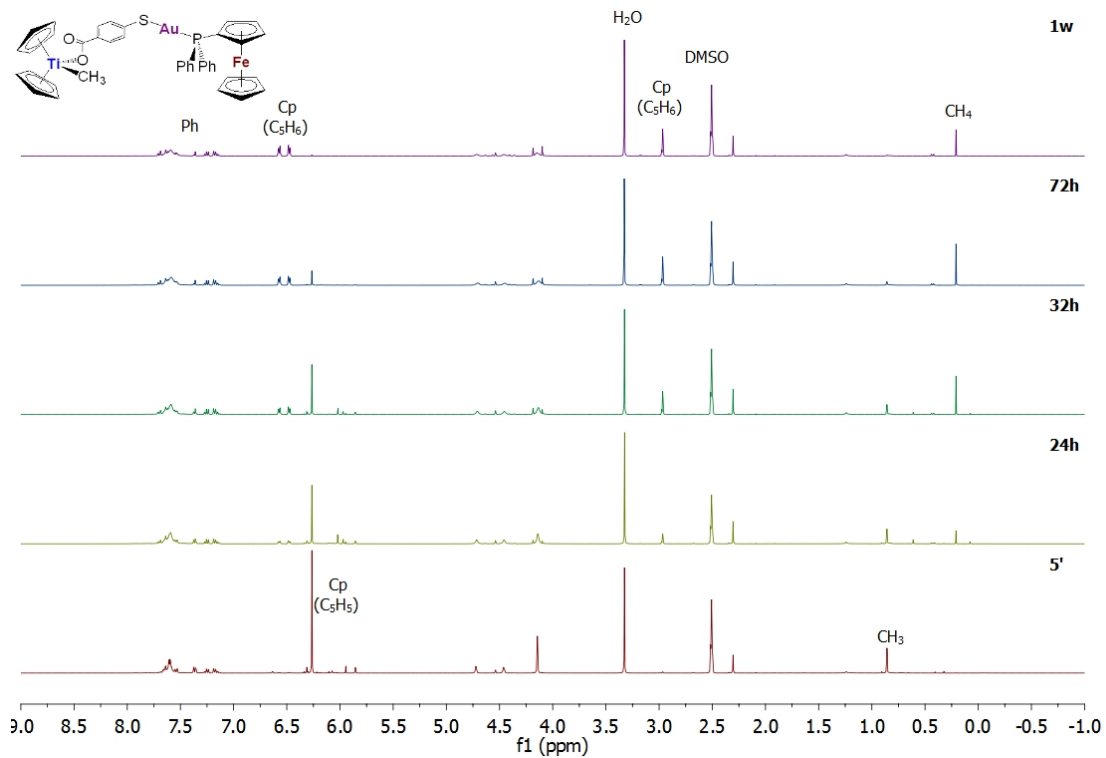


Figure S14. ^1H NMR spectrum in $\text{DMSO}-d_6$. Decomposition of compound 7 over time. $t_{1/2}=36\text{h}$.

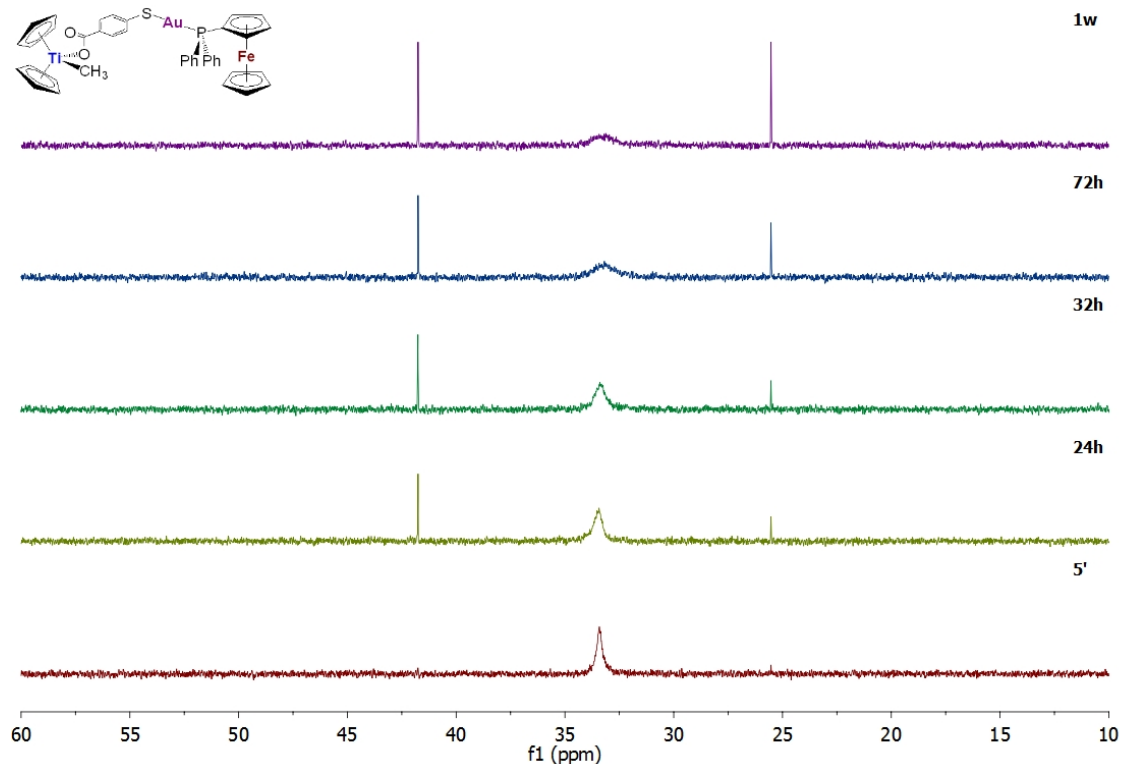


Figure S15. $^{31}\text{P}\{\text{H}\}$ NMR spectrum in $\text{DMSO}-d_6$. Decomposition of compound 7 over time. $t_{1/2}=36\text{h}$.

3. UV-visible spectra of compound **4**, **5**, **6** and **7** in different solvents

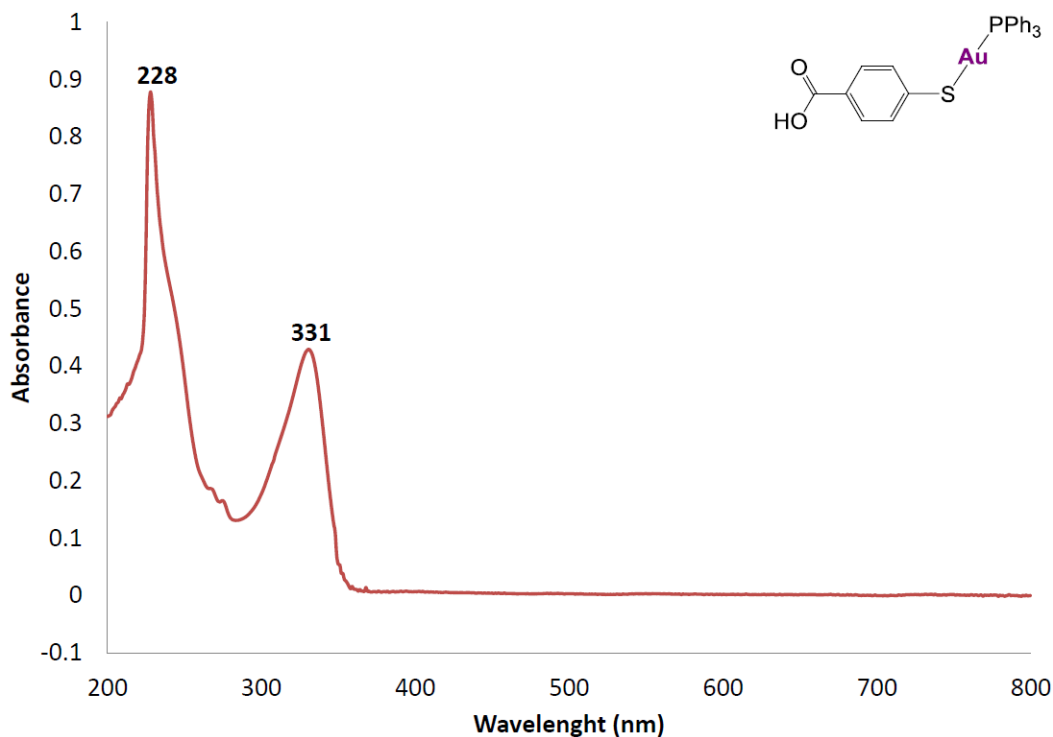


Figure S16. UV-visible spectrum of compound **4** ($2.33 \cdot 10^{-5}$ M) in dichloromethane.

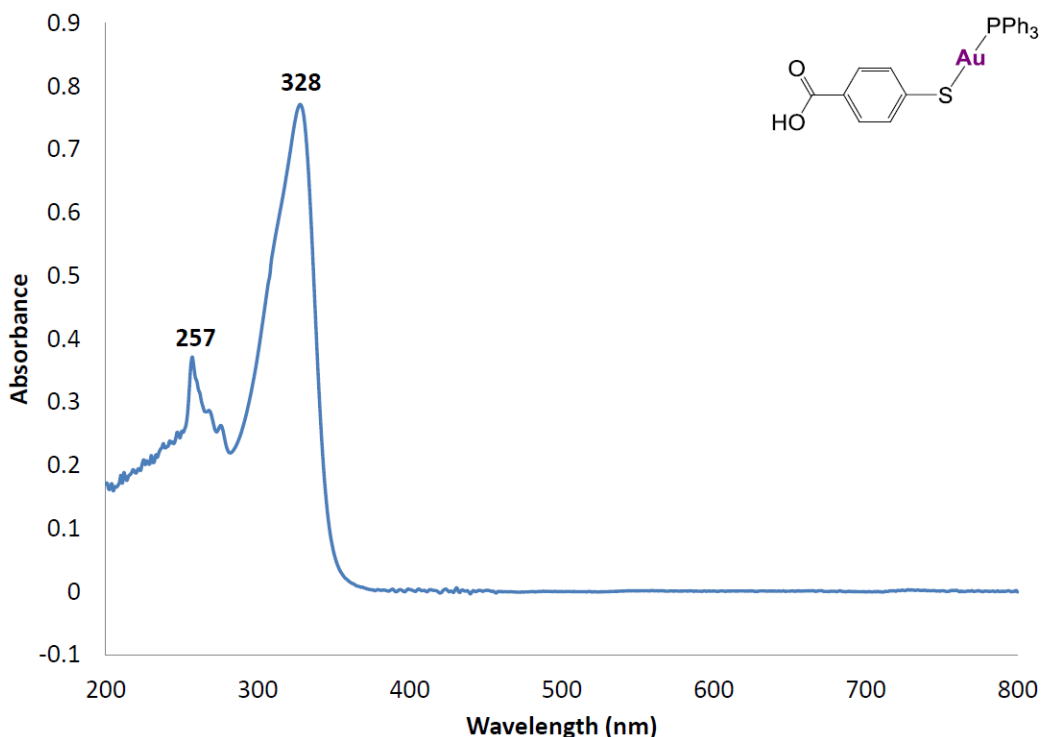


Figure S17. UV-visible spectrum of compound **4** ($2.33 \cdot 10^{-5}$ M) in DMSO.

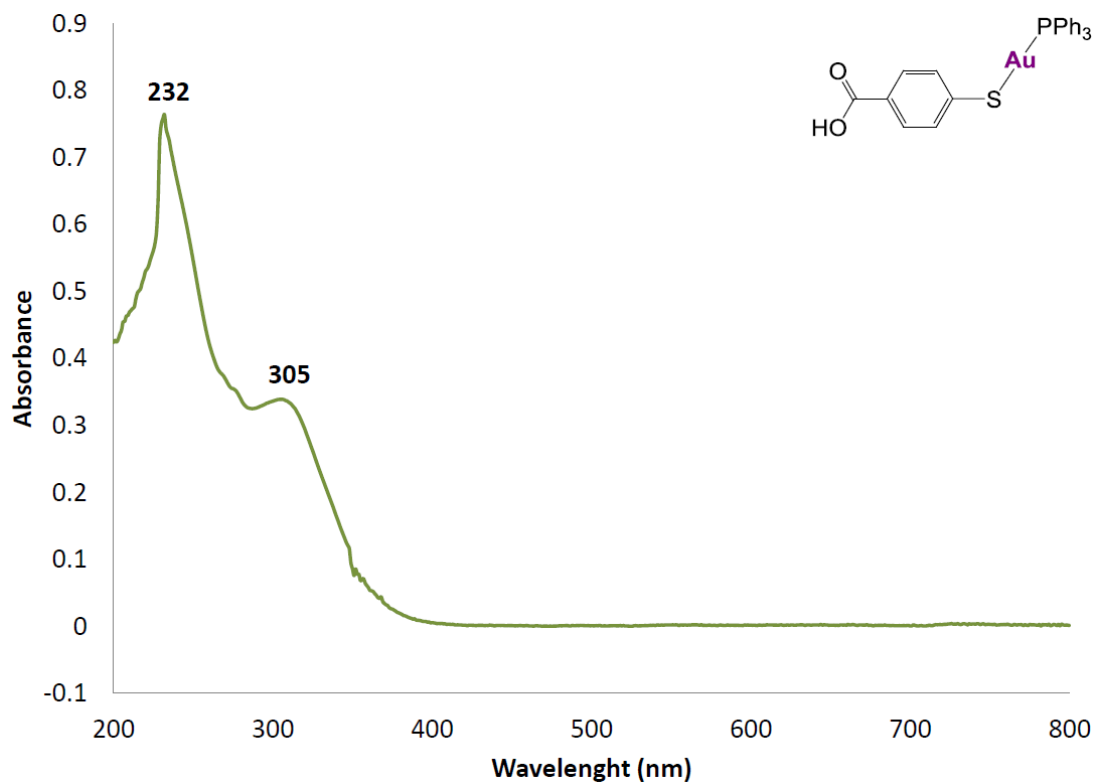


Figure S18. UV-visible spectrum of compound **4** ($2.33 \cdot 10^{-5} \text{ M}$) in 1:99 DMSO/PBS-1X (pH 7.4).

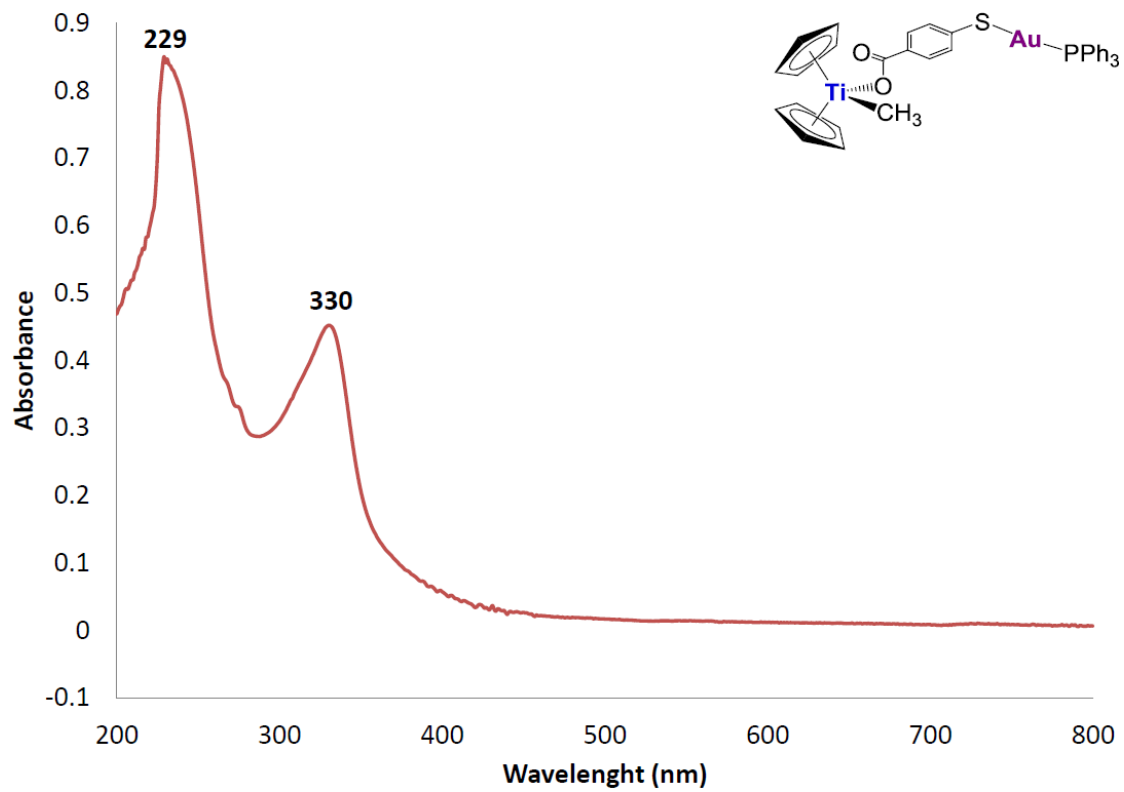


Figure S19. UV-visible spectrum of compound **5** ($2.35 \cdot 10^{-5} \text{ M}$) in dichloromethane.

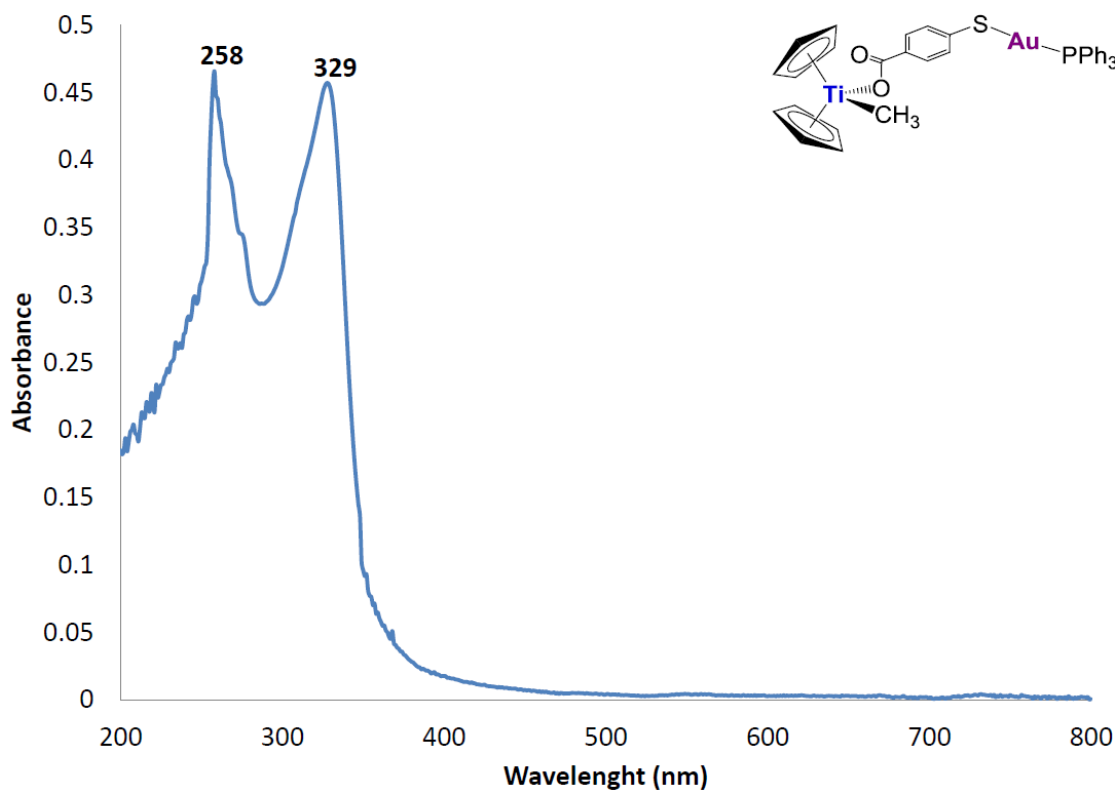


Figure S20. UV-visible spectrum of compound **5** ($2.35 \cdot 10^{-5}$ M) in DMSO.

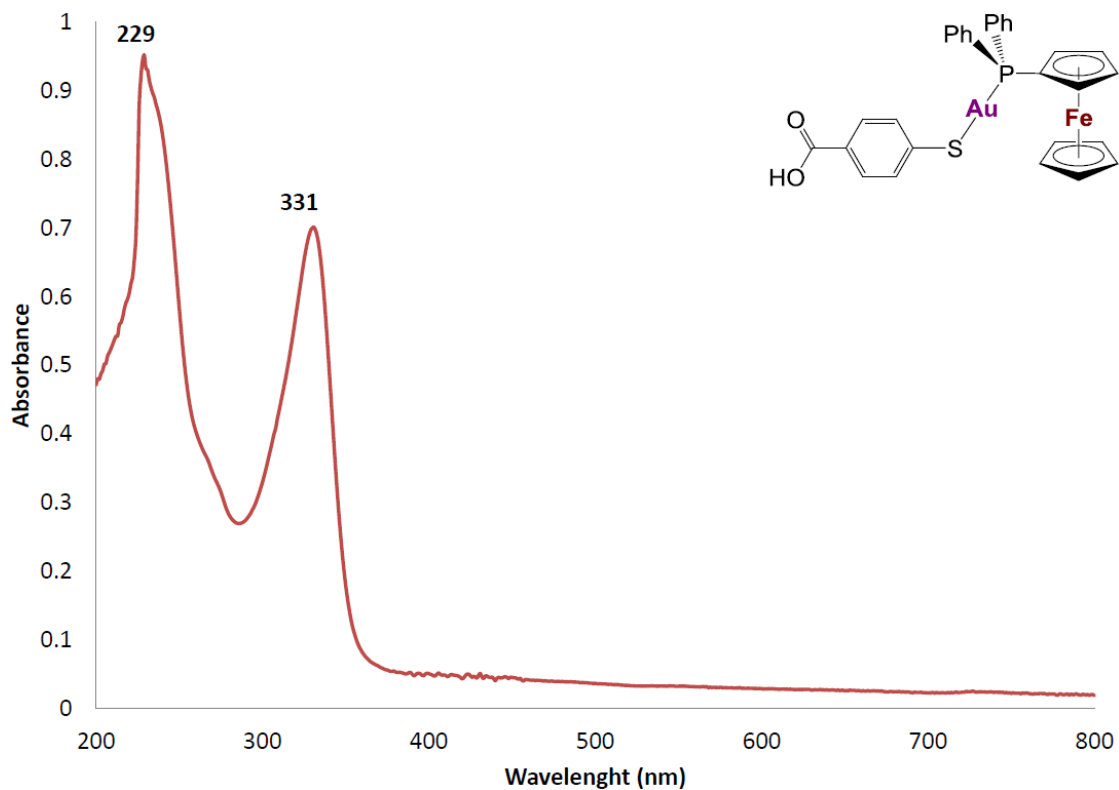


Figure S21. UV-visible spectrum of compound **6** ($3.34 \cdot 10^{-5}$ M) in dichloromethane.

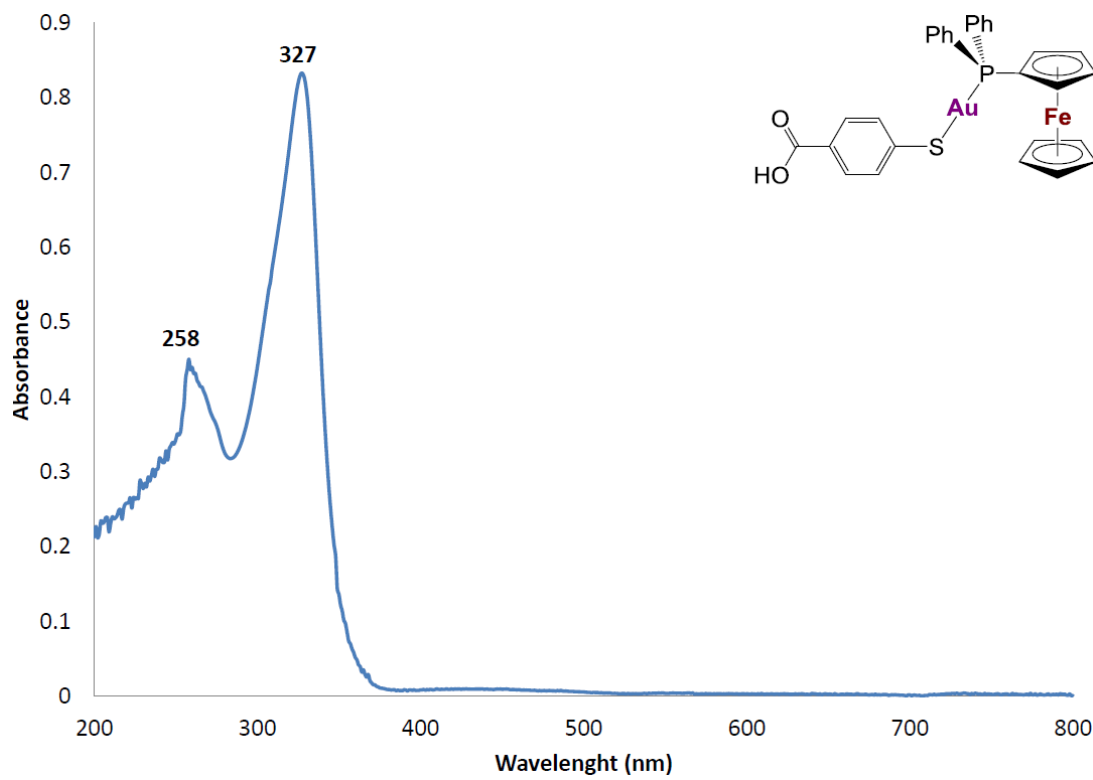


Figure S22. UV-visible spectrum of compound **6** ($3.34 \cdot 10^{-5}$ M) in DMSO.

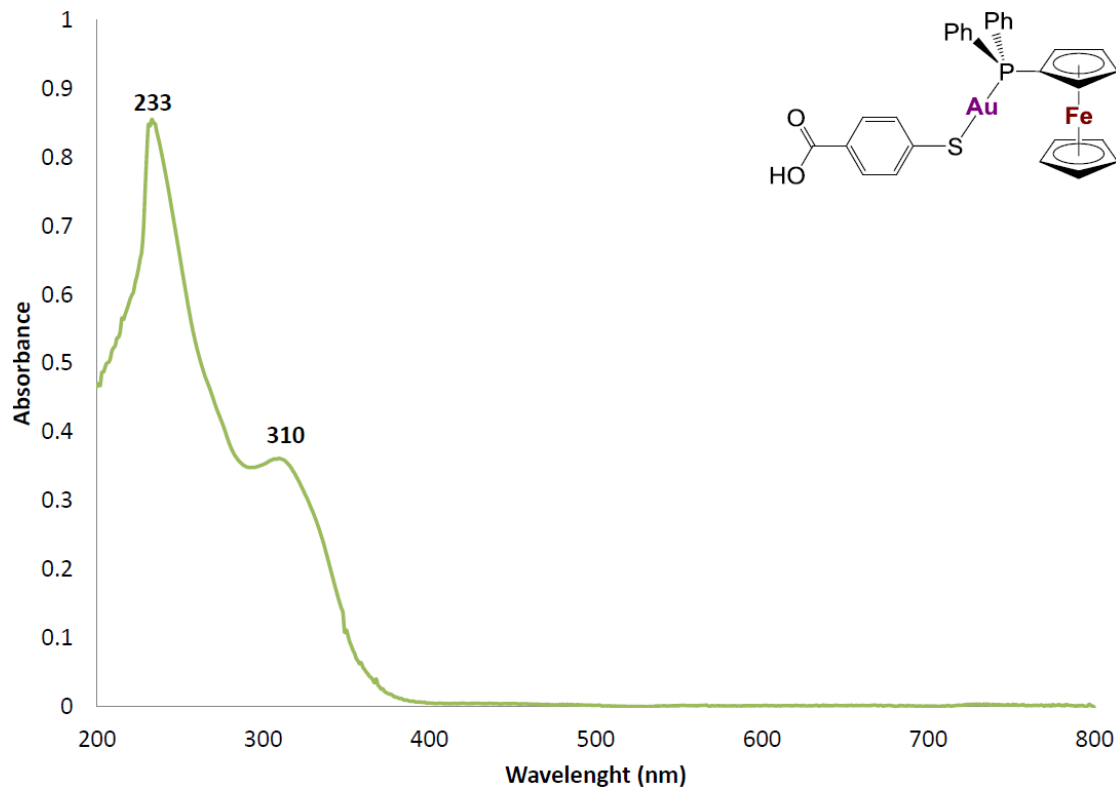


Figure S23. UV-visible spectrum of compound **6** ($3.34 \cdot 10^{-5}$ M) in 1:99 DMSO/PBS-1X (pH 7.4).

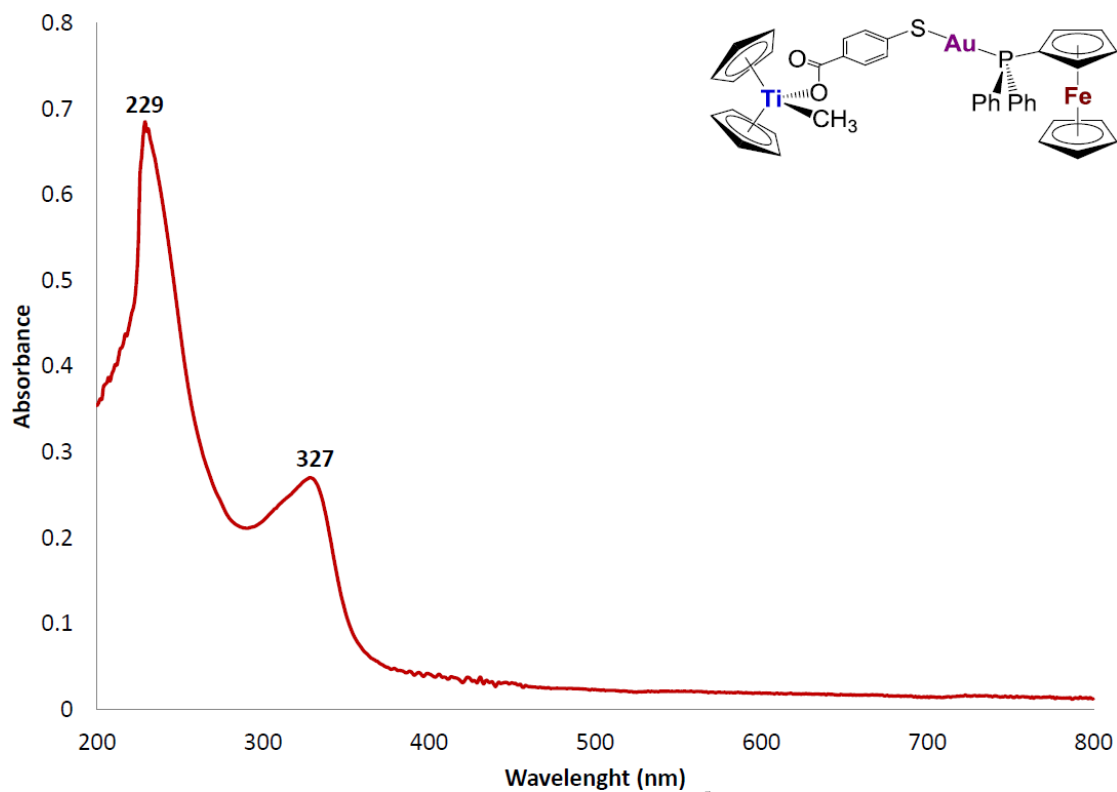


Figure S24. UV-visible spectrum of compound 7 ($3.42 \cdot 10^{-5}$ M) in dichloromethane.

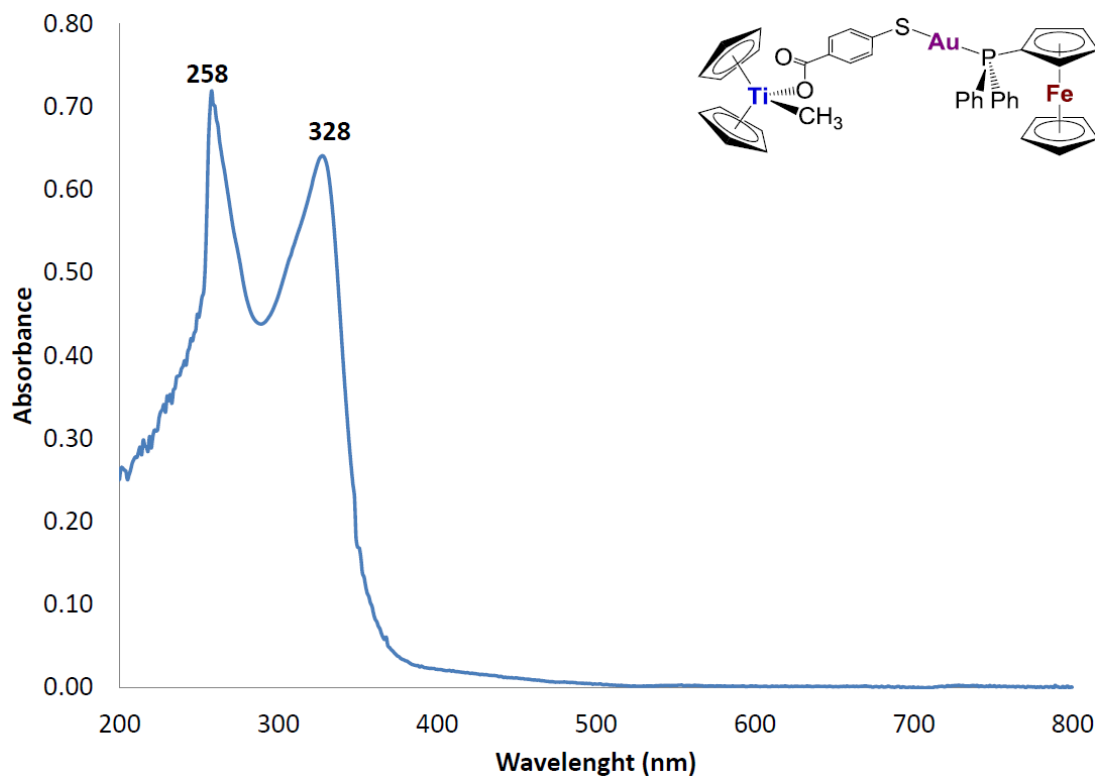


Figure S25. UV-visible spectrum of compound 7 ($3.42 \cdot 10^{-5}$ M) in DMSO.

4. Selected UV-visible spectra of decomposition of compounds **5 and **7** in 1:99 DMSO/PBS-1X**

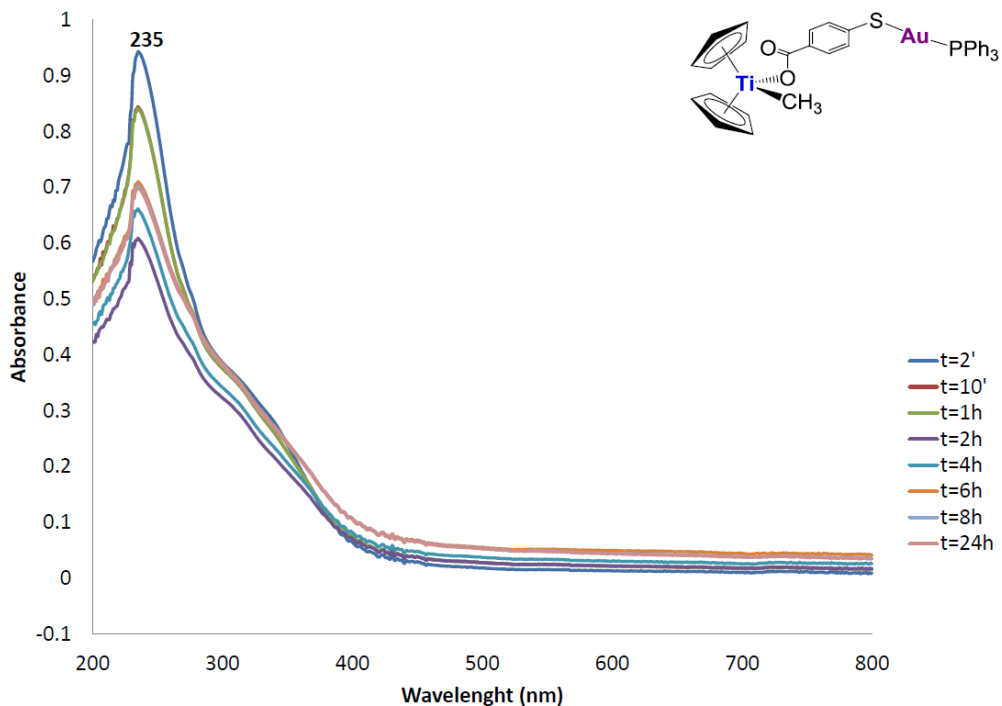


Figure S26. UV-visible spectrum of compound **5** ($2.35 \cdot 10^{-5}$ M) in 1:99 DMSO/PBS-1X (pH 7.4) recorded over time, incubation at RT.

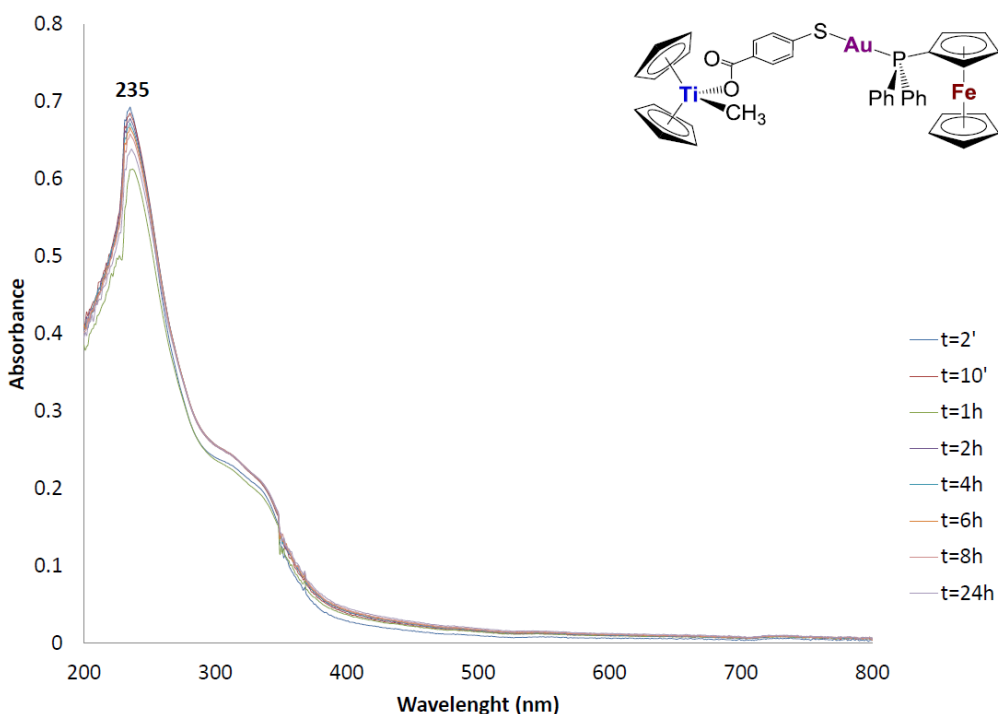


Figure S27. UV-visible spectrum of compound **7** ($3.42 \cdot 10^{-5}$ M) in 1:99 DMSO/PBS-1X (pH 7.4) recorded over time, incubation at RT.

5. Solid state IR spectra of compounds **4**, **5**, **6** and **7**

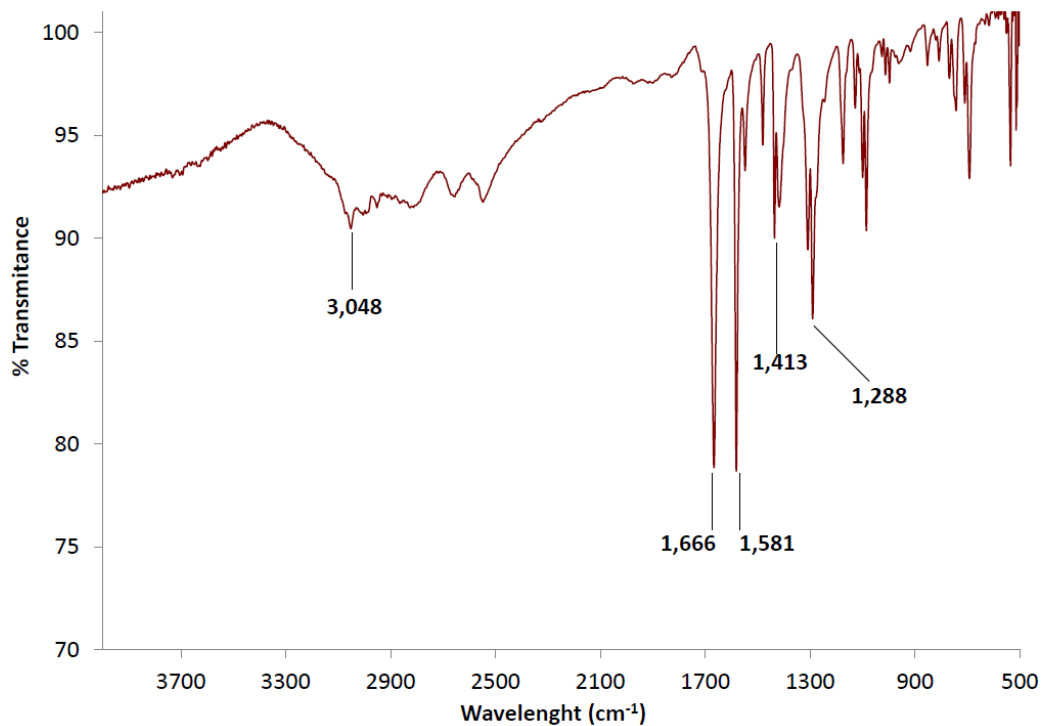


Figure S28. IR spectrum of compound **4** in solid state at RT.

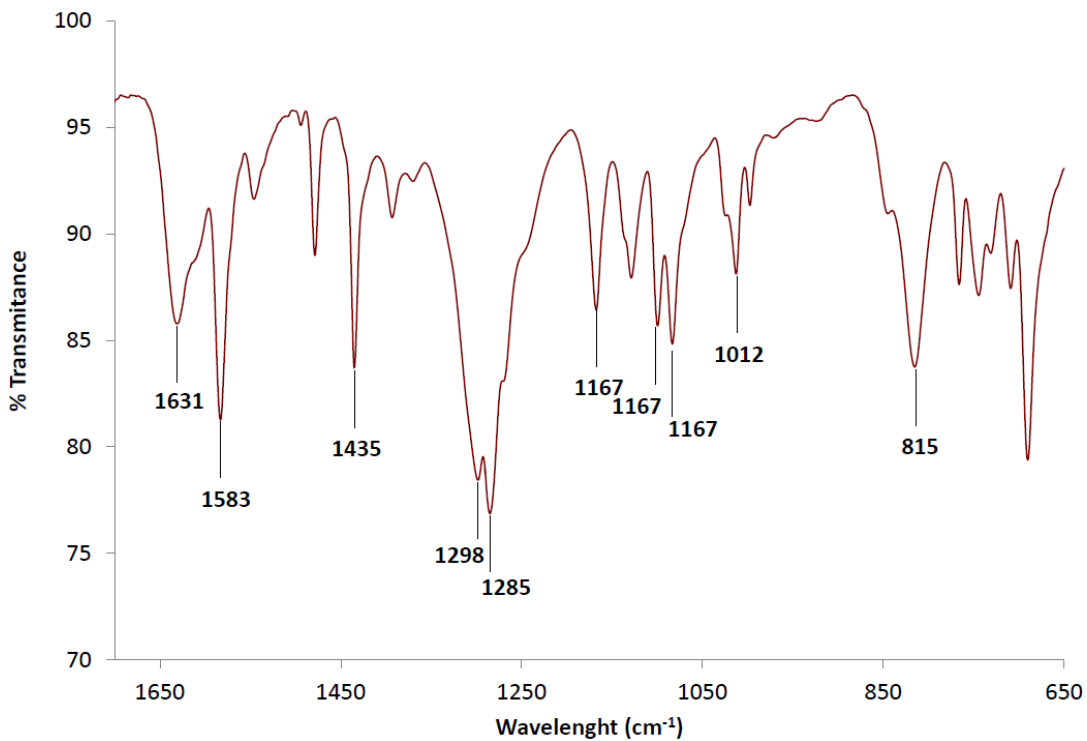


Figure S29. IR spectrum of compound **5** in solid state at RT.

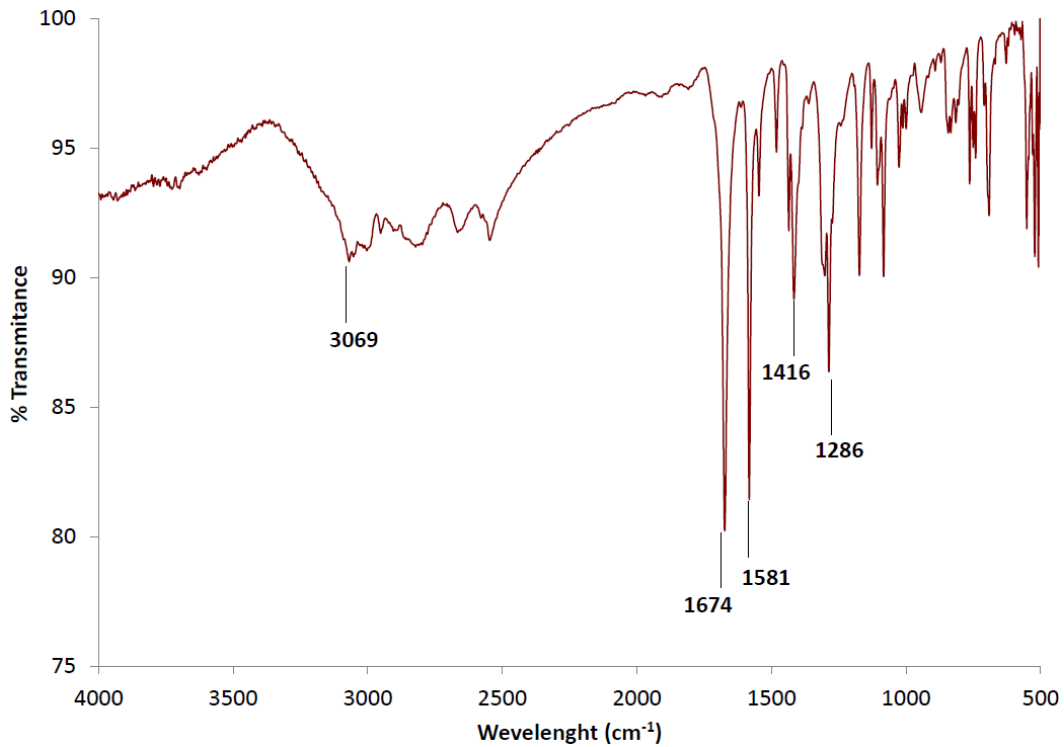


Figure S30. IR spectrum of compound **6** in solid state at RT.

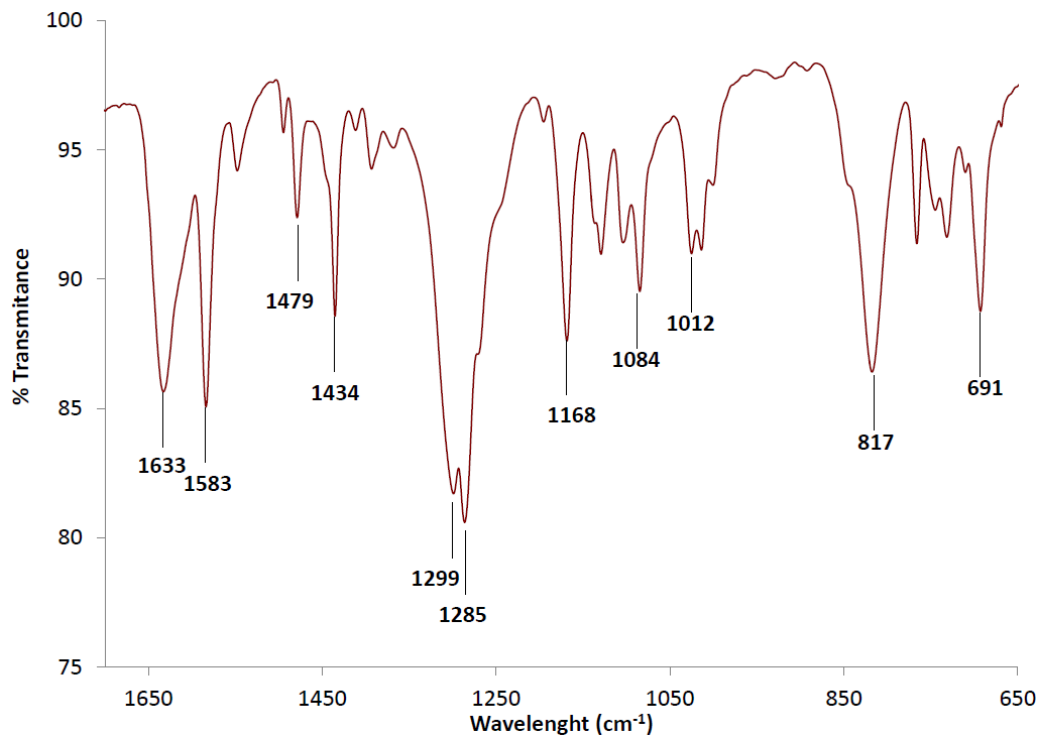


Figure S31. IR spectrum of compound **7** in solid state at RT.

6. ESI+ mass spectra of compounds **5** and **7** and theoretical isotopic distributions of relevant peaks

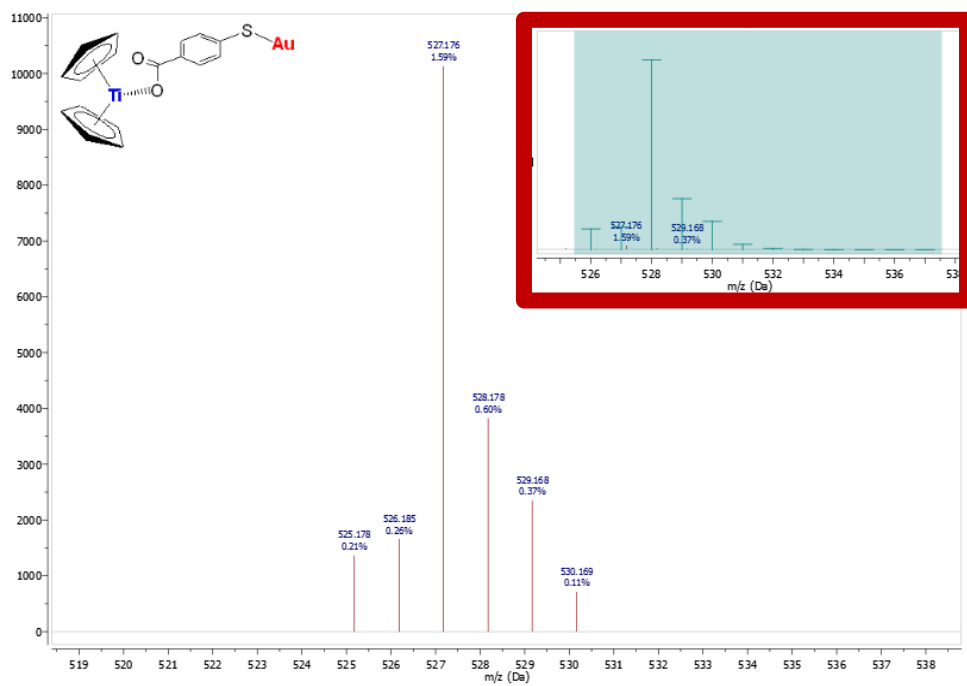


Figure S32. Magnification of peak at $[m/z]$: 527.1 $[\text{Cp}_2\text{Ti}\{\text{OOC-}p\text{-C}_6\text{H}_4\text{-S-Au}\}]^+$ in MS ESI+ of compound **5** in 1%DMSO-PBS solution at $t=0\text{h}$. Insert: theoretical isotopic distribution.

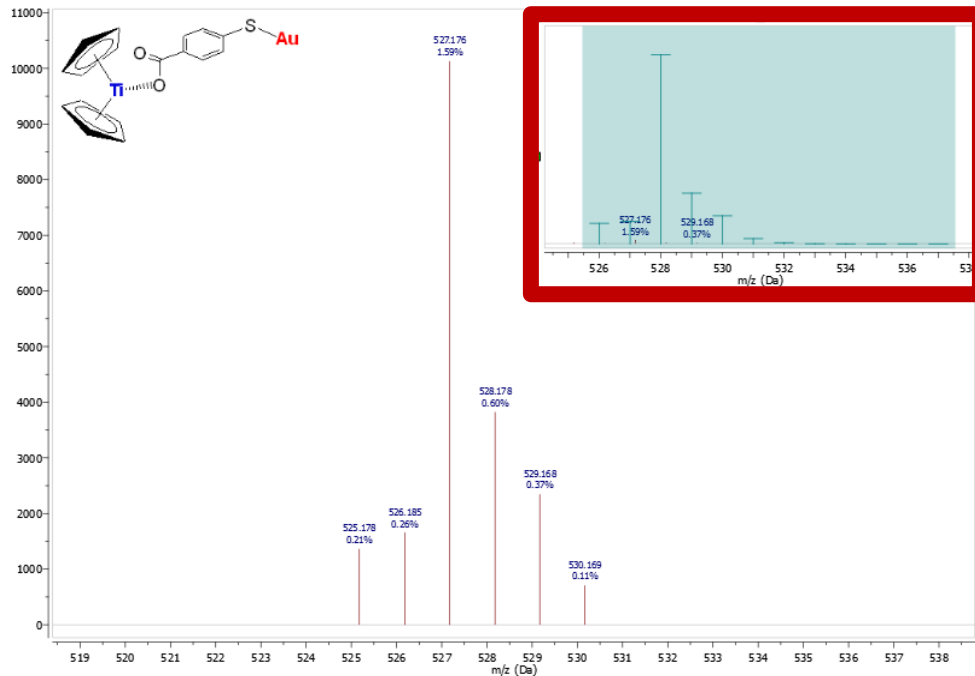


Figure S33. Magnification of peak at $[m/z]$: 527.1 $[\text{Cp}_2\text{TiMe}\{\text{OOC-}p\text{-C}_6\text{H}_4\text{-S-Au}\}]^+$ in MS ESI+ of compound **5** in 1%DMSO-PBS solution at $t=24\text{h}$. Insert: theoretical isotopic distribution.

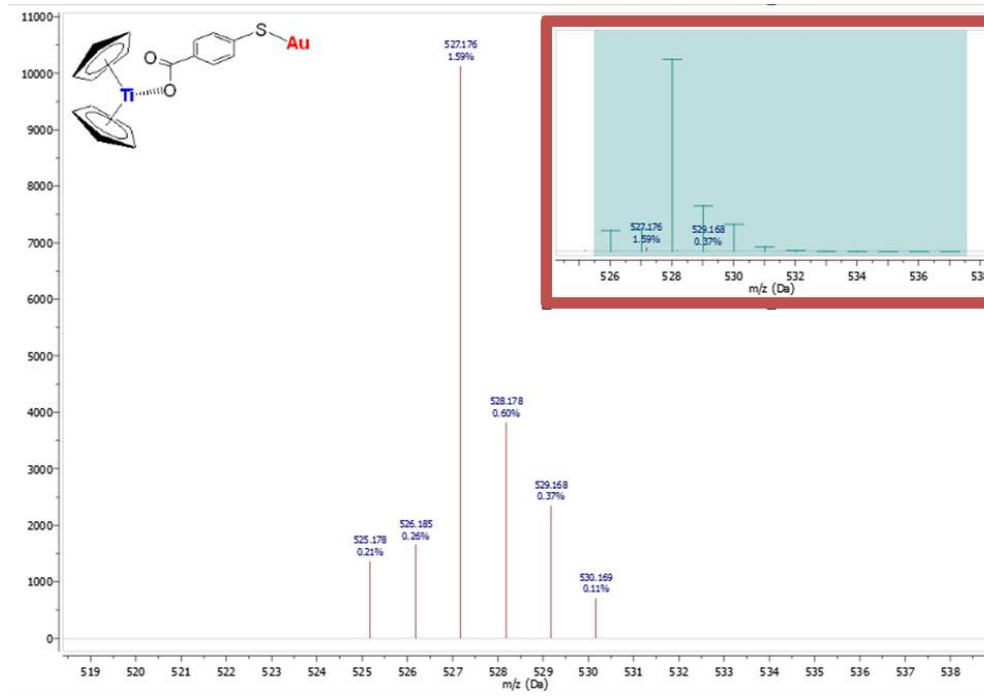


Figure S34. Magnification of peak at $[m/z]$:527.2 $[\text{Cp}_2\text{Ti}\{\text{OOC}-p\text{-C}_6\text{H}_4\text{-S-Au}\}]^+$ in MS ESI+ of compound 7 in 1%DMSO-PBS solution at $t=0\text{h}$. Insert: theoretical isotopic distribution.

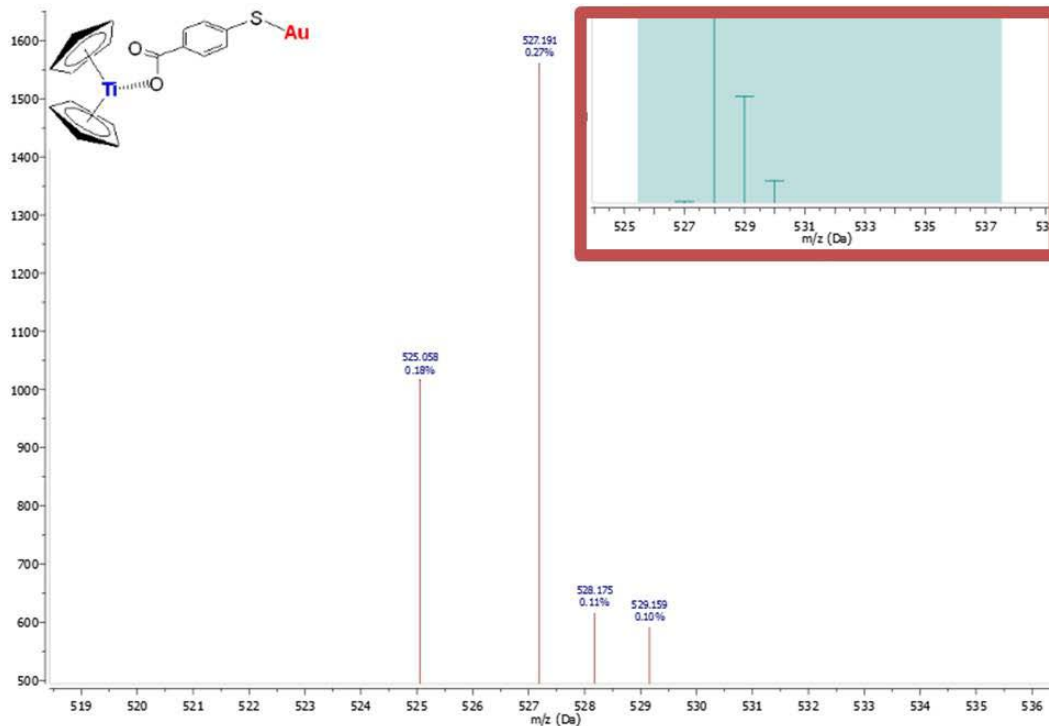


Figure S35. Magnification of peak at $[m/z]$:527.2 $[\text{Cp}_2\text{Ti}\{\text{OOC}-p\text{-C}_6\text{H}_4\text{-S-Au}\}]^+$ in MS ESI+ of compound 7 in 1%DMSO-PBS solution at $t=24\text{h}$. Insert: theoretical isotopic distribution.

7. Crystallographic data for compound **6**

Table S1. Crystal Data and Structure Refinement for compound **6**.

formula	C ₂₉ H ₂₄ AuFeO ₂ PS
fw	720.33
T [K]	293 (2)
λ (Mo _{Kα})[Å]	0.71073
crystal system	Triclinic
space group	P-1
<i>a</i> [Å]	9.18700(10)
<i>b</i> [Å]	9.9640(2)
<i>c</i> [Å]	15.5540(3)
α [°]	108.4110(11)
β [°]	96.8050(12)
γ [°]	95.3800(12)
V [Å] ³	1328.34(4)
Z	2
D _{calcd} (g cm ⁻³)	1.801
μ (mm ⁻¹)	6.225
GOF	1.104
R ₁ [<i>I</i> > 2σ]	0.0331
wR ₂ (all data)	0.0846

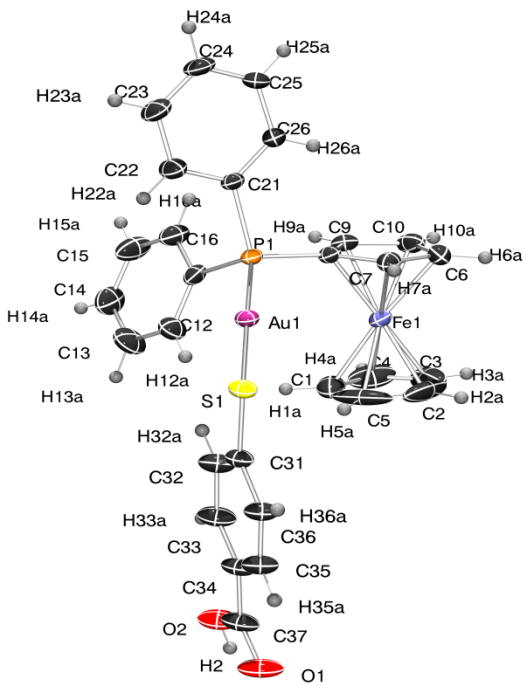


Figure S36. ORTEP view of the molecular structure of **6** showing the complete labelling scheme.

Table S2. Selected Structural Parameters of complex **6** obtained from X-ray single crystal diffraction studies. Bond lengths in Å and angles in °.

Au(1)-P(1)	2.2647(15)	P(1)-Au(1)-S(1)	177.31(5)
Au(1)-S(1)	2.3128(16)	P(1)-C(8)-Fe(1)	128.7(3)
distance Fe-Z (centroid of C ₅ H ₄)	1.640	Au(1) -S(1)- C(31)	105.1(2)
distance Fe-Z' (centroid of C ₅ H ₅)	1.667	Z-Fe(1)-Z'	175.86
P(1)-C(8)	1.789(6)	C(8)-P(1)-C(21)	104.7(3)
P(1)-C(11)	1.823(6)	C(8)-P(1)-C(11)	108.0(3)
P(1)-C(21)	1.822(6)	C(21)-P(1)-C(11)	103.2(3)
S(1)-C(31)	1.770(6)	C(8)-P(1)-Au(1)	112.38(19)
Fe(1)-C(1)	2.023(10)	C(21)-P(1)-Au(1)	115.2(2)
Fe(1)-C(2)	1.987(10)	C(11)-P(1)-Au(1)	112.6(2)
Fe(1)-C(3)	2.004(10)		
Fe(1)-C(4)	2.028(10)		
Fe(1)-C(5)	2.000(9)		
Fe(1)-C(6)	2.042(7)		
Fe(1)-C(7)	2.034(6)		
Fe(1)-C(8)	2.029(5)		
Fe(1)-C(9)	2.048(6)		
Fe(1)-C(10)	2.046(7)		

8. DFT Studies for compounds **4**, **5**, **6** and **7**

The calculations have been performed using the hybrid density functional method B3LYP,⁴ as implemented in Gaussian09.⁵ Geometries were optimized with the 6-311G(d) basis set for the P and S elements, the 6-31G(d,p) basis set for the C, N, P, S, and H elements and the SDD pseudopotential for the titanium, iron and gold metal centers.⁶ Frequency calculations have been done at the same level of theory as the geometry optimizations to confirm the nature of the stationary points.

8.1. Comparison of Selected Geometrical Properties

Table S3. Comparison of Selected Geometrical Properties of Compounds **4^a**, **5^a**, **6^a**, **6^b** and **7^a**. Bond lengths in Å and angles in °.

	4^a	5^a	6^a	6^b	7^a
Ti-O _{coordinanted}	-	1.902	-	-	1.899
Ti-O _{non coordinanted}	-	3.516	-	-	3.510
Ti-Z _{average}	-	2.098	-	-	2.099
Au-S	2.354	2.353	2.356	2.3128(16)	2.353
Au-P	2.339	2.336	2.338	2.2647(15)	2.339
Fe-Z _{centroid of C5H4}	-	-	1.686	1.640	1.685
Fe-Z' _{centroid of C5H5}	-	-	1.692	1.667	1.690
O-Ti-CH ₃	-	93.06	-	-	93.09
Z-Ti-Z	-	133.33	-	-	133.26
P-Au-S	177.33	178.59	176.26	177.31(5)	177.89
Au-S-C	106.03	101.82	104.88	105.1(2)	105.51
P-C-Fe	-	-	128.68	128.7(3)	127.80
Z-Fe-Z'	-	-	177.48	175.86	177.50

^a DFT Optimized Structures.

^b X-Ray Structure.

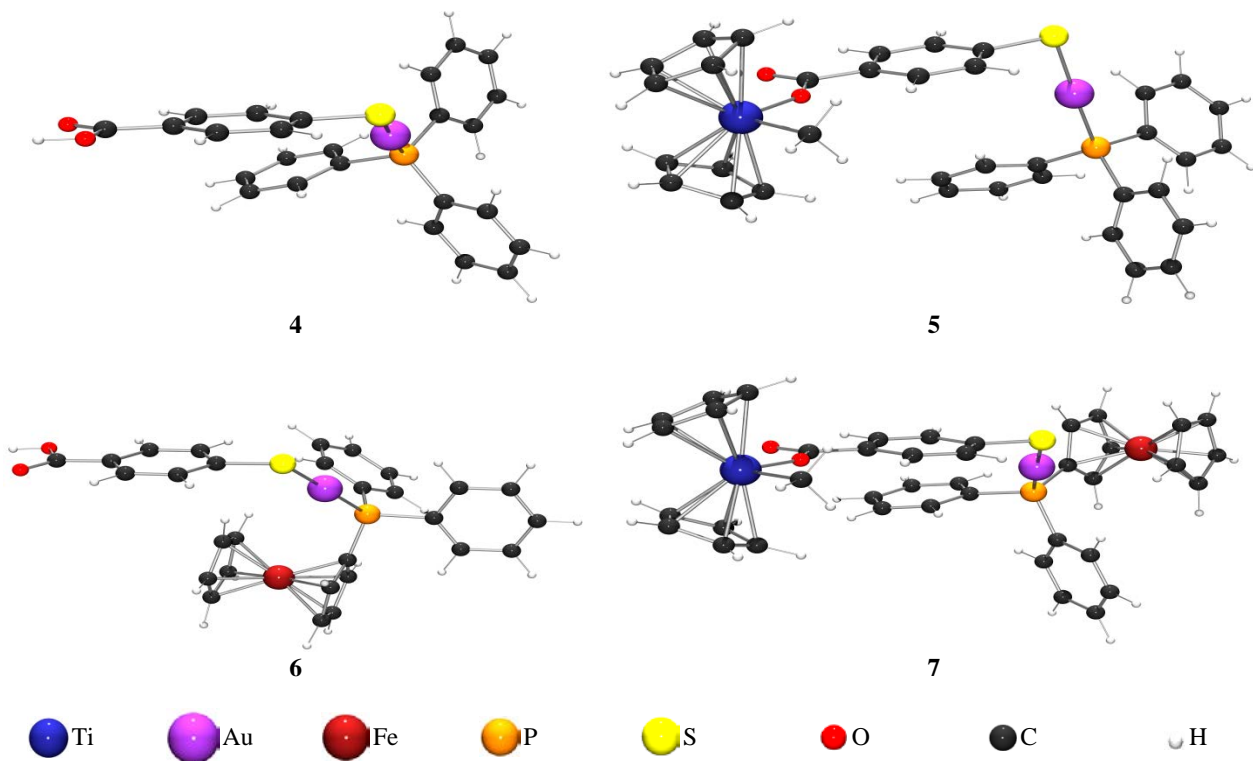


Figure S37. Optimized Structures of Compounds **4**, **5**, **6**, and **7**.

8.2. Optimized geometries and cartesian coordinates of stationary points

Compound **4**

Charge: 0

Multiplicity: 1

79	0.085625	-1.064996	-0.134123
15	-1.887698	0.179041	0.034797
16	2.015271	-2.405718	-0.272852
6	6.866511	1.245631	0.047397
8	6.882395	2.408337	-0.316597
6	5.696936	0.345366	-0.016001
6	4.498682	0.845545	-0.547535
6	5.737243	-0.983789	0.433251
6	3.369967	0.041595	-0.630540
1	4.476779	1.871758	-0.900245
6	4.604914	-1.785995	0.361692
1	6.657634	-1.381519	0.846621
6	3.397688	-1.289639	-0.168588
1	2.455990	0.435400	-1.064145
1	4.643098	-2.808228	0.724801
6	-1.575658	1.986834	0.043579
6	-3.049939	-0.126145	-1.351769
6	-2.837054	-0.164335	1.566733
6	-2.400781	2.896262	-0.634502
6	-0.466934	2.465920	0.762012
6	-2.516463	-0.398381	-2.622473
6	-4.442832	-0.087757	-1.184799
6	-3.588875	0.825562	2.218257
6	-2.810667	-1.466432	2.092427
1	-3.251964	2.540308	-1.205904
6	-2.123453	4.264152	-0.586910
6	-0.198732	3.833053	0.810875
1	0.188989	1.768154	1.275695
1	-1.439500	-0.452506	-2.755865
6	-3.363605	-0.612254	-3.709327
6	-5.286009	-0.308567	-2.275238
1	-4.870177	0.103617	-0.205709
6	-4.310331	0.512232	3.371605
1	-3.602679	1.840930	1.834688
6	-3.538122	-1.775184	3.241373
1	-2.211298	-2.232554	1.608285
1	-2.764906	4.960639	-1.118827
6	-1.026115	4.733864	0.135798
1	0.662513	4.192190	1.366062
1	-2.940672	-0.824388	-4.686653
6	-4.748806	-0.567929	-3.537231
1	-6.362726	-0.281443	-2.135788
6	-4.288252	-0.786750	3.882232
1	-4.885474	1.285504	3.872371

1	-3.508415	-2.784170	3.641494
1	-0.810574	5.797795	0.167058
1	-5.407579	-0.743293	-4.382674
1	-4.846953	-1.026306	4.782212
8	7.975954	0.652017	0.567632
1	8.662031	1.338705	0.553723

Compound **5**, monodentate

Charge: 0

Multiplicity: 1

22	-6.818661	0.449263	-0.310292
79	2.602378	-1.300342	-0.293623
15	4.179158	0.398183	0.003399
16	1.058233	-3.043198	-0.628504
6	-4.282889	-0.600058	1.058847
8	-5.100749	-0.271194	0.070225
8	-4.572874	-0.446057	2.243086
6	-6.884156	2.760179	-1.041929
1	-7.011822	2.984030	-2.090835
6	-5.649535	2.569605	-0.372415
1	-4.671613	2.569074	-0.834019
6	-5.922482	2.293483	0.988643
1	-5.199540	2.028996	1.747605
6	-7.324840	2.293630	1.159398
1	-7.845752	2.114982	2.088663
6	-7.923052	2.584810	-0.098151
1	-8.981518	2.676482	-0.296942
6	-8.454618	-0.535005	1.159074
1	-8.668723	-0.074502	2.112574
6	-7.483155	-1.534558	0.929223
1	-6.779525	-1.902742	1.662684
6	-7.518726	-1.870166	-0.444287
1	-6.848297	-2.554817	-0.945321
6	-8.529787	-1.092352	-1.063854
1	-8.800733	-1.117658	-2.109237
6	-9.108968	-0.263308	-0.075075
1	-9.916606	0.438114	-0.229164
6	-6.517503	0.338551	-2.450212
1	-5.632165	0.934363	-2.694795
1	-6.313794	-0.706629	-2.704321
1	-7.353608	0.689567	-3.064682
6	-2.975981	-1.176821	0.620135
6	-2.039694	-1.552431	1.595170
6	-2.658510	-1.360359	-0.733203
6	-0.814327	-2.097132	1.226679
1	-2.298315	-1.415405	2.640150
6	-1.429819	-1.902092	-1.103728

1	-3.380497	-1.073781	-1.490568	1	-6.824754	2.836229	-2.129591
6	-0.486915	-2.273380	-0.130541	6	-5.378424	2.473655	-0.473895
1	-0.099951	-2.399863	1.985798	1	-4.431956	2.396635	-0.991085
1	-1.188284	-2.040470	-2.152736	6	-5.578414	2.363567	0.927964
6	3.894748	1.386132	1.523132	1	-4.813066	2.159273	1.661095
6	5.891775	-0.247121	0.140058	6	-6.958575	2.457056	1.183115
6	4.215160	1.612211	-1.373033	1	-7.430073	2.385514	2.153080
6	4.948646	1.882592	2.304954	6	-7.623551	2.642781	-0.062257
6	2.569113	1.651252	1.905725	1	-8.687571	2.764325	-0.210393
6	6.092383	-1.462982	0.815061	6	-7.846768	-0.479806	1.732910
6	6.996169	0.429222	-0.399708	1	-7.637473	-0.084417	2.716759
6	4.492142	2.972457	-1.167182	6	-7.198685	-1.586765	1.132847
6	3.962548	1.151057	-2.675577	1	-6.379284	-2.141224	1.564660
1	5.977503	1.670887	2.031737	6	-7.730508	-1.763238	-0.159437
6	4.678132	2.640231	3.446241	1	-7.393320	-2.482894	-0.892056
6	2.305138	2.414373	3.042381	6	-8.745359	-0.786590	-0.353916
1	1.745985	1.251231	1.319793	1	-9.348781	-0.665834	-1.240953
1	5.240330	-2.005174	1.215875	6	-8.826115	-0.005495	0.820014
6	7.378051	-1.982646	0.960132	1	-9.510762	0.812941	0.990422
6	8.280645	-0.099431	-0.257180	6	5.346788	0.349174	-1.344003
1	6.855589	1.360662	-0.938550	6	5.806225	1.501761	-1.999389
6	4.525066	3.853202	-2.249901	1	5.411993	2.476474	-1.729772
1	4.671353	3.347148	-0.164413	6	6.763206	1.398741	-3.010756
6	4.003506	2.034039	-3.754114	1	7.109761	2.295563	-3.515897
1	3.723329	0.104053	-2.840513	6	7.268380	0.149570	-3.374880
1	5.499966	3.016454	4.048459	1	8.009549	0.072383	-4.164967
6	3.358979	2.909166	3.814221	6	6.811593	-1.001948	-2.729903
1	1.276877	2.610939	3.330598	1	7.193073	-1.977111	-3.017320
1	7.521272	-2.924360	1.481443	6	5.851360	-0.905536	-1.723423
6	8.473684	-1.302161	0.423909	1	5.483297	-1.805095	-1.237711
1	9.128934	0.428793	-0.682610	6	3.222653	2.009516	-0.209318
6	4.284212	3.385764	-3.542896	6	2.109338	2.038552	-1.065898
1	4.735172	4.905221	-2.080439	1	1.780268	1.126415	-1.556099
1	3.804138	1.667461	-4.756617	6	1.417492	3.230095	-1.278949
1	3.151880	3.495385	4.704729	1	0.556691	3.240464	-1.940708
1	9.473627	-1.712670	0.529524	6	1.821548	4.400276	-0.632035
1	4.306534	4.074211	-4.382619	1	1.276306	5.325811	-0.792021
				6	2.920025	4.376349	0.228486
				1	3.232399	5.282293	0.739617
				6	3.620510	3.187312	0.440969
				1	4.467690	3.176937	1.119162
				6	-7.119277	0.308415	-2.310988
				1	-6.281344	0.751047	-2.854384
				1	-7.172532	-0.749547	-2.577853
				1	-8.051307	0.804640	-2.604620
				6	-2.969642	-1.284333	-0.014319
				6	-2.233661	-1.373949	1.177083
				6	-2.420464	-1.793201	-1.200393
				6	-0.970055	-1.954497	1.180210
				1	-2.667499	-0.986951	2.093496
				6	-1.155818	-2.374119	-1.196327

Compound 5, bidentate

Charge: 0

Multiplicity: 1

79	2.649779	-1.408014	0.016550
22	-6.662928	0.438944	-0.154752
16	1.197662	-3.261105	-0.006941
15	4.108849	0.417356	0.009086
6	-4.311604	-0.660022	-0.017226
8	-4.982580	-0.532738	-1.097814
8	-4.853433	-0.225175	1.046478
6	-6.640404	2.683843	-1.078135

1	-2.996661	-1.726107	-2.117428	1	0.312609	5.086124	0.603612
6	-0.407304	-2.454511	-0.008570	1	-0.757796	5.073182	-1.873721
1	-0.405145	-2.030959	2.103726	1	3.082721	2.737021	0.320384
1	-0.732762	-2.769072	-2.114371	1	4.579975	1.433121	3.969664
6	5.081687	0.594747	1.555357	1	1.351368	2.984731	-3.681021
6	6.386291	1.112086	1.564424	1	2.635289	1.472322	5.516870
6	4.487166	0.207676	2.767630	1	4.302972	0.643657	1.645819
6	7.078338	1.249188	2.769017	1	6.478463	-0.851048	-1.884752
1	6.866049	1.398475	0.633911	1	4.431649	0.434511	-1.363948
6	5.180976	0.352372	3.968703	1	-0.228026	2.709340	1.756707
1	3.486469	-0.215480	2.766745	1	-1.965553	2.686885	-2.245947
6	6.476754	0.873111	3.971163	1	0.406663	0.707222	4.723732
1	8.089182	1.646361	2.765673	1	0.822713	0.526581	-2.703520
1	4.712810	0.047643	4.899873	1	6.692608	-3.213354	-1.144947
1	7.019164	0.977276	4.906305	1	-1.651809	1.230950	-0.007486
				1	0.123342	-0.080204	2.390631
				1	4.837539	-4.289090	0.114369
				1	2.781422	-3.014854	0.625168
				1	-7.658854	1.426113	1.735165
				1	-4.538886	0.145190	2.040977
				1	-2.500676	-1.167723	1.538375
6	2.413409	3.319757	-1.736297	1	-6.372841	-1.306395	-1.553295
6	-0.263539	4.282870	0.164384	1	-4.312625	-2.595948	-2.088397
6	-0.829714	4.276137	-1.146018	8	-6.795213	0.985789	1.681981
6	2.588486	2.474253	-0.604220	8	-7.817916	0.266377	-0.188849
6	1.677491	2.598560	-2.724746	79	0.027007	-1.598582	-0.237952
6	3.601399	1.114258	3.622857	26	0.563598	2.745507	-0.964755
6	2.508419	1.135181	4.492316	15	1.932984	-0.290703	0.113184
6	-0.549202	3.025328	0.773895	15	1.932984	-0.290703	0.113184
6	3.442976	0.675038	2.308024	16	-1.831311	-2.961698	-0.724738
6	-1.467355	3.014550	-1.343683				
6	1.958356	1.211885	-0.891045				
6	1.388532	1.304787	-2.209484				
6	5.674682	-1.322656	-1.326894				
6	4.519823	-0.594652	-1.031208				
6	1.256036	0.707858	4.046993				
6	-1.295836	2.241276	-0.158673	22	8.008466	-0.104945	0.264567
6	2.183721	0.257524	1.848594	79	-1.879117	-0.681641	0.223337
6	1.094066	0.267222	2.732302	26	-6.110011	-1.280779	-0.656951
6	5.794621	-2.649034	-0.911081	15	-3.512530	0.967665	-0.052621
6	3.473274	-1.194697	-0.316274	16	-0.287367	-2.380900	0.562595
6	4.753582	-3.253710	-0.202071	6	5.138707	0.057254	-0.802631
6	3.595788	-2.534223	0.089456	8	6.135163	-0.285081	0.001231
6	-4.486855	-0.452235	1.137181	8	5.290356	0.802057	-1.768806
6	-3.338873	-1.181822	0.848725	6	8.744041	1.380928	2.033035
6	-6.834409	0.262311	0.528896	1	9.100075	0.964401	2.963981
6	-5.589797	-0.492765	0.270250	6	7.402435	1.728773	1.732799
6	-3.250712	-1.961608	-0.321615	1	6.547558	1.573271	2.376523
6	-5.515394	-1.279808	-0.888685	6	7.362447	2.234951	0.412570
6	-4.364756	-2.000008	-1.182817	1	6.478279	2.521049	-0.139494
1	2.742561	4.347385	-1.814000	6	8.671999	2.181805	-0.114252

Compound 7

Charge: 0
Multiplicity: 1

1	8.963777	2.501395	-1.103959	6	-3.644546	3.076623	-1.956282
6	9.531548	1.657092	0.891222	6	-1.589607	2.891970	-0.685032
1	10.599081	1.511053	0.806613	6	-7.125994	0.152226	-1.777590
6	9.194933	-0.273678	-1.830729	1	-6.721102	1.393601	0.042266
1	9.416285	0.617690	-2.399187	6	-6.247690	-0.595083	-2.619882
6	8.034451	-1.067843	-1.964816	1	-4.029354	-0.901957	-2.532162
1	7.185599	-0.835459	-2.592503	6	-7.537190	-2.508949	0.214894
6	8.131662	-2.140080	-1.045861	6	-6.712703	-3.266231	-0.671552
1	7.369299	-2.884037	-0.859348	6	-6.698463	-1.944500	1.223289
6	9.362181	-2.019303	-0.353562	6	-5.364710	-3.172143	-0.211032
1	9.728167	-2.684500	0.414703	6	-5.357523	-2.357994	0.959933
6	10.020260	-0.862126	-0.832723	6	-5.322001	3.383433	2.769514
1	10.987784	-0.503978	-0.510361	1	-4.913601	3.488926	0.661736
6	8.006471	-1.351441	2.032440	6	-4.521951	1.409313	3.912958
1	7.336892	-0.893132	2.767387	1	-3.478094	-0.028080	2.693343
1	7.598353	-2.328058	1.752783	6	-3.122003	4.182981	-2.629771
1	8.984980	-1.503609	2.500788	1	-4.638524	2.716453	-2.202092
6	3.816312	-0.534726	-0.445916	6	-1.075784	4.000934	-1.355606
6	2.704506	-0.240962	-1.249902	1	-0.982565	2.381591	0.057992
6	3.644713	-1.379064	0.660853	1	-8.202623	0.204427	-1.869103
6	1.456152	-0.777517	-0.959343	1	-6.542746	-1.207845	-3.460920
1	2.845361	0.406185	-2.109603	1	-8.604705	-2.362547	0.119641
6	2.392608	-1.907280	0.961937	1	-7.047023	-3.793912	-1.554599
1	4.498813	-1.610284	1.288803	1	-7.017647	-1.297664	2.029145
6	1.275278	-1.614500	0.159067	1	-4.495520	-3.612989	-0.679763
1	0.608791	-0.561067	-1.602566	1	-4.478103	-2.081988	1.525055
1	2.268145	-2.547334	1.829864	6	-5.180178	2.639893	3.943629
6	-4.969458	0.416399	-0.972900	1	-5.821688	4.347517	2.791488
6	-4.162202	1.652323	1.524185	1	-4.394974	0.834467	4.825505
6	-2.882415	2.425161	-0.975328	6	-1.840923	4.647426	-2.329518
6	-6.346947	0.776693	-0.762158	1	-3.717201	4.678073	-3.391602
6	-4.921090	-0.443252	-2.126970	1	-0.073850	4.351117	-1.126349
6	-4.814323	2.895297	1.565394	1	-5.571501	3.024478	4.880937
6	-4.010481	0.918516	2.710351	1	-1.435571	5.505140	-2.858213

8.3. Calculated IR spectra of compounds **4**, **5**, **6** and **7**

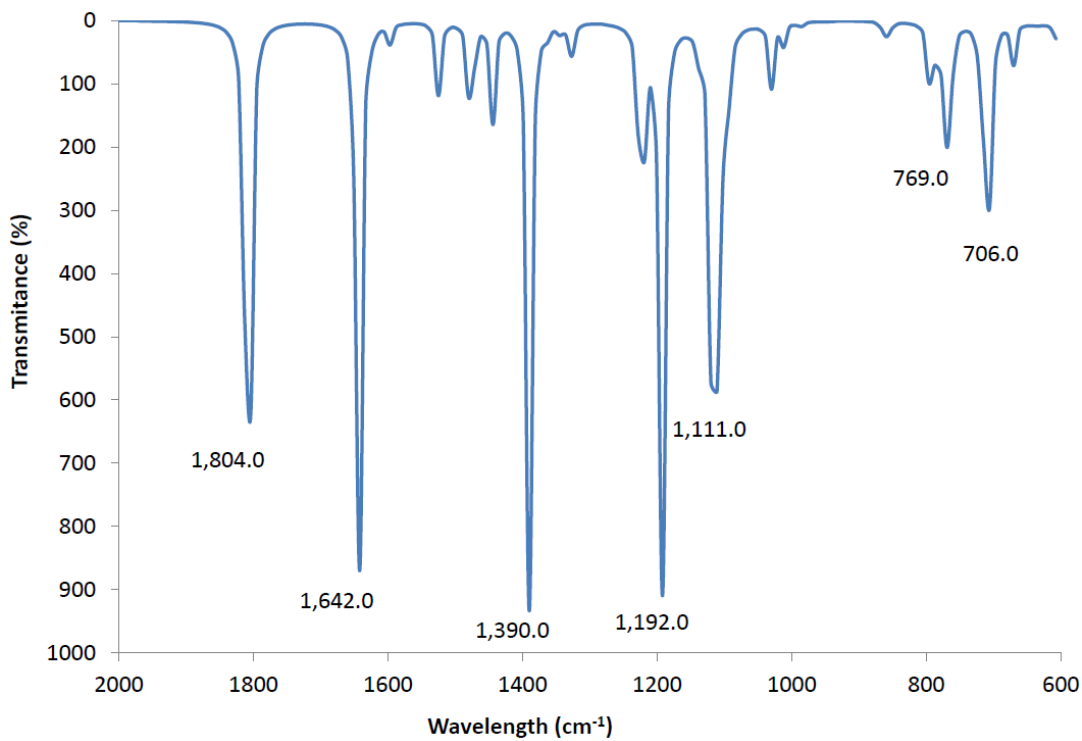


Figure S38. Calculated IR spectrum of compound **4**.

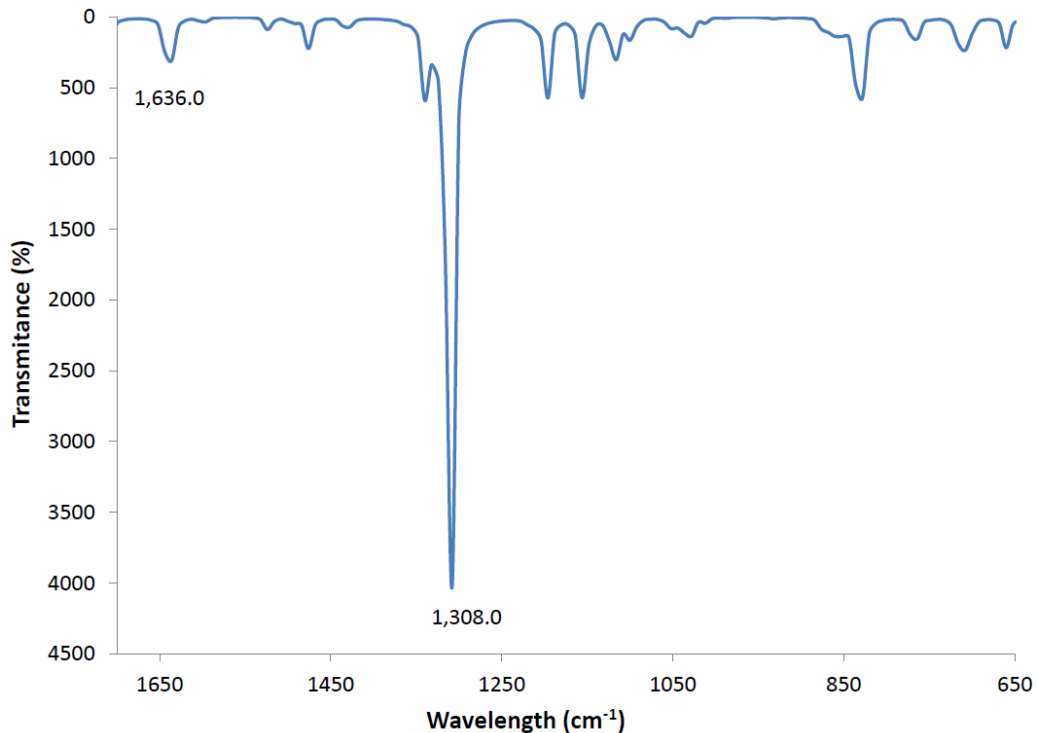


Figure S39. Calculated IR spectrum of compound **5** monodentate.

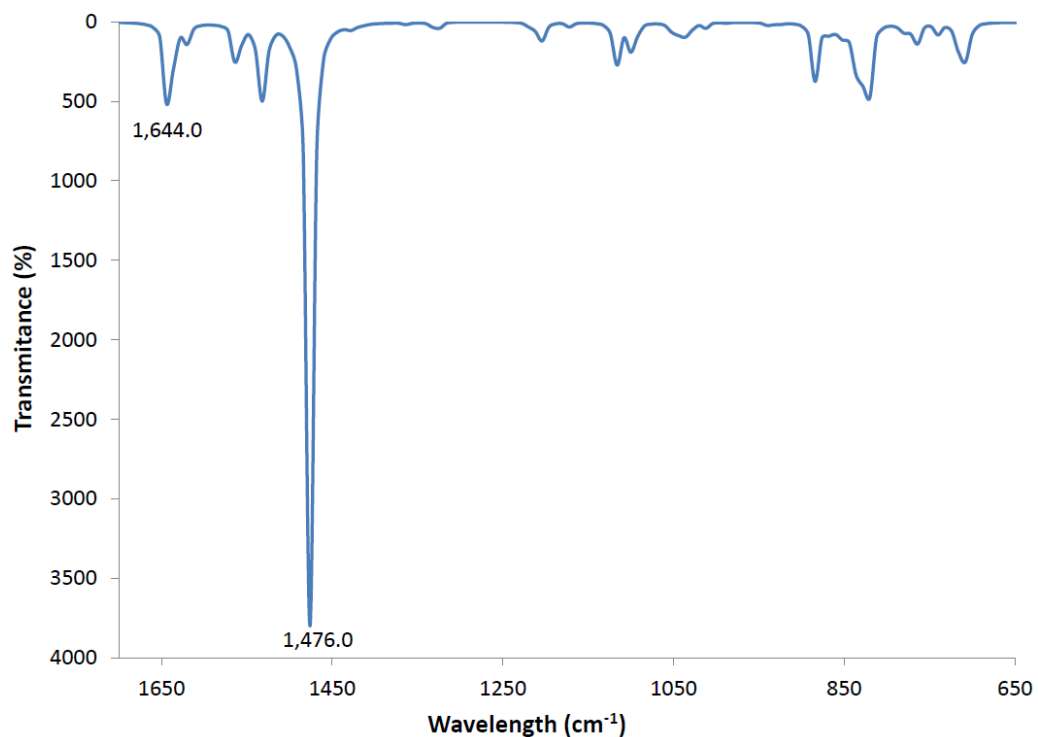


Figure S40. Calculated IR spectrum of compound **5** bidentate.

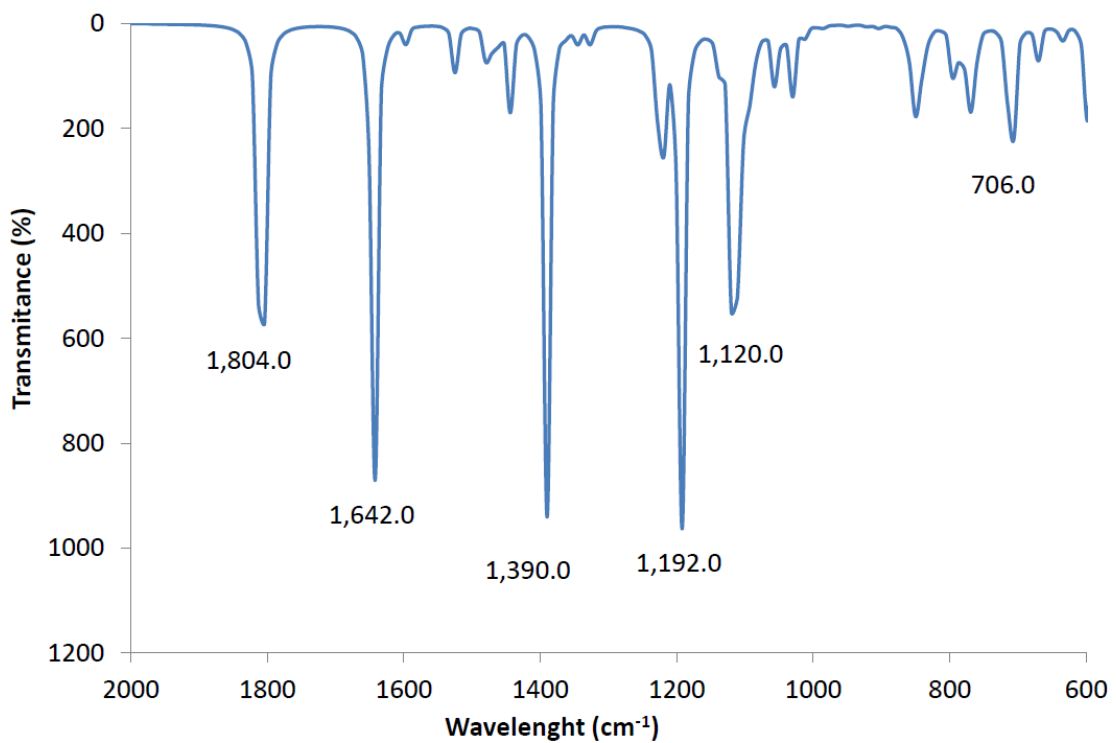


Figure S41. Calculated IR spectrum of compound **6**.

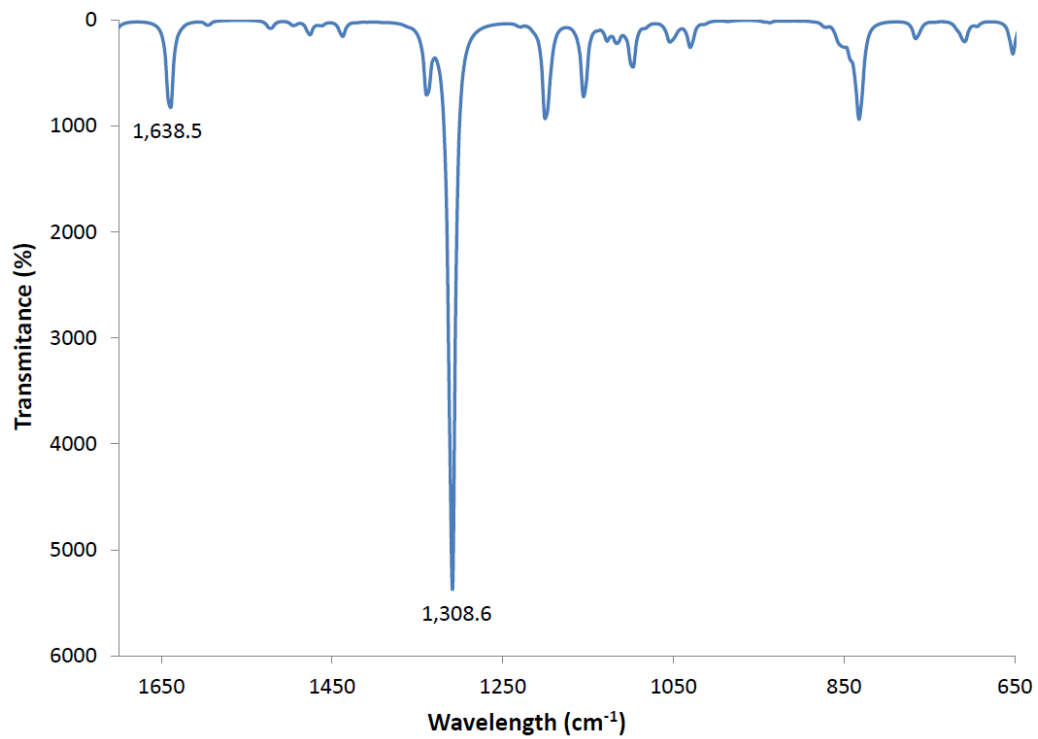


Figure S42. Calculated IR spectrum of compound 7.

9. Cytotoxicity Assays (IC_{50} values after 24 and 72 hours of treatment)

Complete cytotoxicity table (including assays at 24 hours) for the new heterometallic TiAu complexes **5** and **7**, monometallic **4** and **6** gold derivatives and cisplatin, titanocene dichloride and Titanocene Y as control compounds

Table S4 IC_{50} values (μM) in human cell lines were determined with heterometallic TiAu compounds $[(\eta-C_5H_5)_2 TiMe(\mu-mba)Au(PR_3)]$ **5** and **7** monometallic $[Au(Hmba)PR_3]$ **4** and **6**, cisplatin, titanocene dichloride, and Titanocene Y. All compounds were dissolved in 1% of DMSO and diluted with water before addition to cell culture medium for a 72 h incubation period. Cisplatin and titanocene dichloride were dissolved in H_2O .

Compound	Time (h)	Caki-1	HEK-293T	RPTC
$[Au(Hmba)(PPh_3)]$ 4	24	18.33 ± 2.24	4.12 ± 0.94	5.25 ± 0.97
	72	2.76 ± 0.35	1.11 ± 0.65	3.87 ± 0.15
Ti-Au 5	24	3.37 ± 0.25	1.67 ± 0.49	3.88 ± 0.86
	72	0.12 ± 0.003	0.49 ± 0.008	2.67 ± 0.12
$[Au(Hmba)MPPF]$ 6	24	4.17 ± 0.87	4.11 ± 0.98	3.91 ± 0.61
	72	3.6 ± 0.342	3.0 ± 0.07	3.78 ± 0.13
Ti-Au 7	24	8.22 ± 1.9	5.11 ± 0.22	4.19 ± 0.11
	72	4.11 ± 0.64	3.09 ± 0.003	3.76 ± 0.21
Cisplatin	24	68.79 ± 0.15	64.42 ± 7.91	46.42 ± 2.46^a
	72	29 ± 4.11	3.27 ± 0.13	^b
$[(\eta-C_5H_5)_2TiCl_2]$	24	> 200	> 200	^b
	72	> 200	> 200	^b
Titanocene Y	24	> 200	> 200	^b
	72	29.42 ± 4.18	> 200	^b

10. Migration assays with compounds **3** and **5**

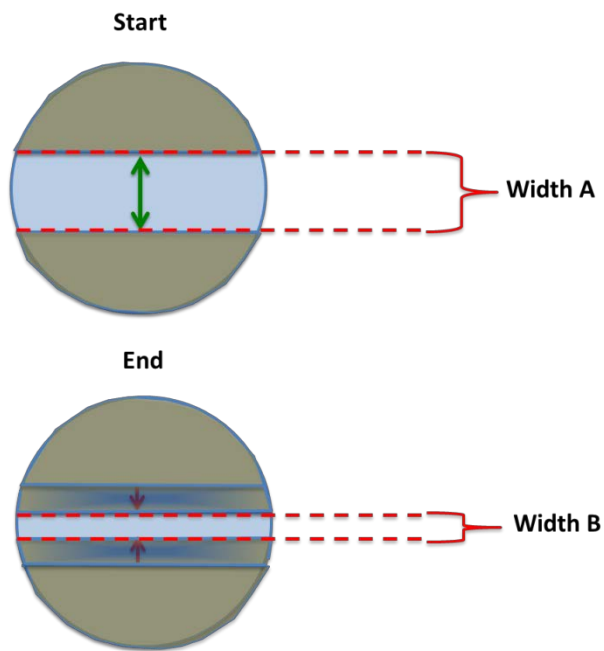


Figure S43. Schematic Representation of Scratch Assay. Tracking cell migration with wound-healing assay. 1) Confluent cell monolayer are wounded with a sterile 10 μ l pipette tip. 2) Then invasion into of the wound gap is observed for 12 hours, and images are captured at 1 hour, 8 hours and 12 hours after the wound under desired treatment condition. 3) Data from four fields of view are then the average of 2 independent experiments. % Migration = [(Area of original wound- Area of wound during healing) /Area of original wound] x100.

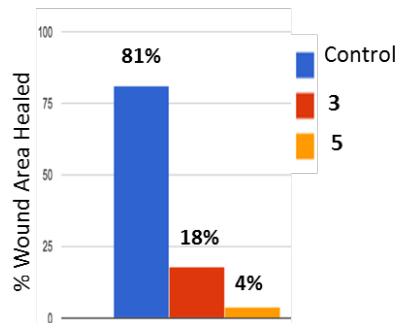


Figure S44. Invasion assay showing that **3** and **5** interfere with Caki-1migration. The bar graph shows the percentage of the wound healed surface. Each bar represents one treatment group, 0.1% DMSO control treated cells blue bar), **3** treated cells (red bar) and **5** treated cells (orange bar). The graph represents results from measurements of the area of the scratch from 4 separate and random fields of view.

11. Inhibition of Thioredoxin Reductase (TrxR) studies of compounds **3, **5** and Auranofin at 5, 12 and 24 h.**

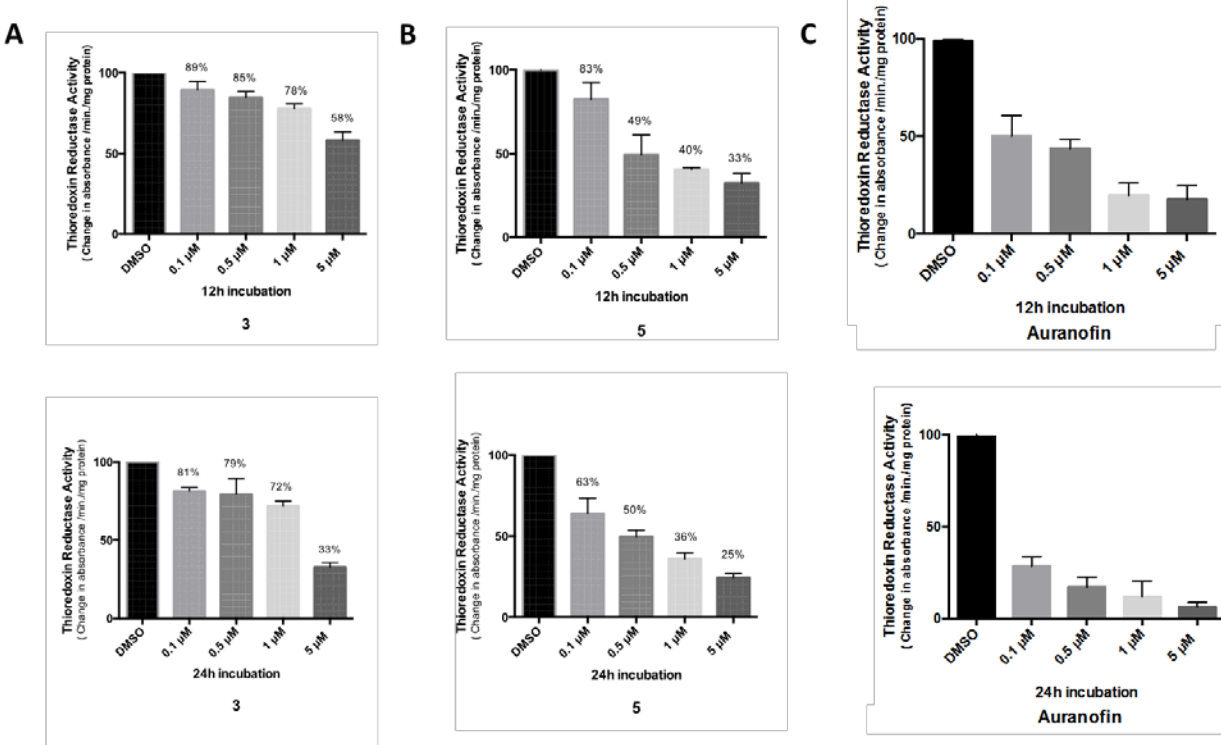


Figure S45. Thioredoxin reductase activity in **3**, **5** or Auranofin treated Caki-1 cells. (A) Activity of endogenous Caki-1 thioredoxin reductase from soluble whole cell lysates following incubation with 1% DMSO or 0.1 μM, 0.5 μM, 1 μM, 5 μM of **3** for 12 hours and 24 hours. (B) Activity of endogenous Caki-1 thioredoxin reductase from soluble whole cell lysates following incubation with 1% DMSO or 0.1 μM, 0.5 μM, 1 μM, 5 μM of **5** for 12 hours and 24 hours. (C) Activity of endogenous Caki-1 thioredoxin reductase from soluble whole cell lysates following incubation with 1% DMSO or 0.1 μM, 0.5 μM, 1 μM, 5 μM of Auranofin for 12 hours and 24 hours.

12. Inhibition studies of a panel of 35 protein kinases of oncological interest of compound 5

Compound 5 was tested against 31 protein kinases at 10 µM ATP (see conditions in the experimental section and reference 70).

The compounds were tested in single dose duplicate mode at a concentration of 1 µM. Control compound staurosporine was tested in 10-dose IC50 mode with 4-fold serial dilution starting at 20 µM. Alternate control compounds were tested in 10-dose IC50 mode with 3-fold serial dilution starting at 20 µM.

Table S5	Compound IC50* (M):					
	Kinase:	Compound 5		Staurosporine	Alternate Control cpd.	Alternate compound ID
		Data 1	Data 2			
AKT1		88.96	88.25	7.13E-09		
AKT2		82.79	82.72	2.26E-08		
AKT3		85.82	85.32	5.04E-09		
ARAF		98.78	98.56		1.54E-08	GW5074
BRAF		102.13	100.62		3.41E-08	GW5074
ERK1		113.99	111.54	1.12E-05		
ERK2/MAPK1		109.42	106.73	7.85E-06		
ERK5/MAPK7		141.72	131.91	1.97E-05		
MAPKAPK2		39.39	39.17	1.19E-07		
MAPKAPK3		42.05	41.54	3.31E-06		
MAPKAPK5/PRAK		96.16	91.73	6.57E-07		
mTOR/FRAP1		111.51	108.67		7.53E-08	PI-103
P38a/MAPK14		119.49	118.95		1.67E-08	SB202190
P38b/MAPK11		121.01	116.03		4.26E-08	SB202190
P38d/MAPK13		97.63	94.42	1.28E-07		
P38g		111.10	110.77	2.45E-07		
p70S6K/RPS6KB1		99.04	98.42	4.82E-10		
PKA		93.37	92.52	1.08E-09		
PKAcg		110.65	103.92	1.46E-08		
PKCa		101.45	96.32	7.64E-10		
PKCb1		93.41	92.87	4.45E-09		
PKCb2		101.06	97.72	1.32E-09		
PKCd		100.17	100.06	6.35E-10		
PKCepsilon		90.79	88.94	1.34E-10		
PKCeta		95.81	95.80	1.48E-09		
PKCg		134.59	132.45	1.47E-09		
PKCiota		99.66	94.98	1.11E-08		
PKCmu/PRKD1		81.55	81.45	1.96E-09		
PKCtheta		80.84	80.53	2.61E-09		
PKCzeta		107.98	105.66	6.37E-08		
RAF1		110.43	109.21		3.75E-08	GW5074

* Empty cells indicate no inhibition or compound activity that could not be fit to an IC50 curve

ND Indicates compound not tested against kinase

Those protein kinases for which there was a significant enzymatic inhibition (>50%) were evaluated for IC₅₀ values. Compounds were tested in a 10-dose IC₅₀ mode with 3-fold serial dilution starting at 100 μM. Compound **5** was dissolved in DMSO and titrated just before use. Control compound staurosporine was tested in 10-dose IC₅₀ mode with 4-fold serial dilution starting at 20 μM.

Table S6	Compound IC₅₀* (M)	
Kinases	Compound 5	Staurosporine
MAPKAPK2	7.88E-07	1.06E-07
MAPKAPK3	3.17E-07	3.88E-06

In the case of lipid protein kinases PI3, compound **5** was tested against 4 PI3K isoforms. Compound **5** was tested in a 10-dose IC₅₀ in singlet with 3-fold serial dilution starting at 200 μM. Control compound, PI-103, was tested in 10-dose IC₅₀ with 3-fold serial dilution starting at 10 μM. The HTRF assay format was used for these PI3Ks. In this case, some precipitation of compound **5** was observed at high concentrations. There was no significant inhibition and the values obtained could not be fit to an IC₅₀ curve.

Table S7	Compound ID IC₅₀* (M)	PI-103 IC₅₀* (M):
Kinases	Compound 5	
PI3Kalpha		6.95E-10
PI3Kbeta		3.89E-09
PI3Kgamma		2.70E-08
PI3Kdelta		1.41E-09

* Empty cells indicate no inhibition or compound activity that could not be fit to an IC₅₀ curve.

13. Effects of Auranofin on MAPKAPK-3 in Caki-1 cells

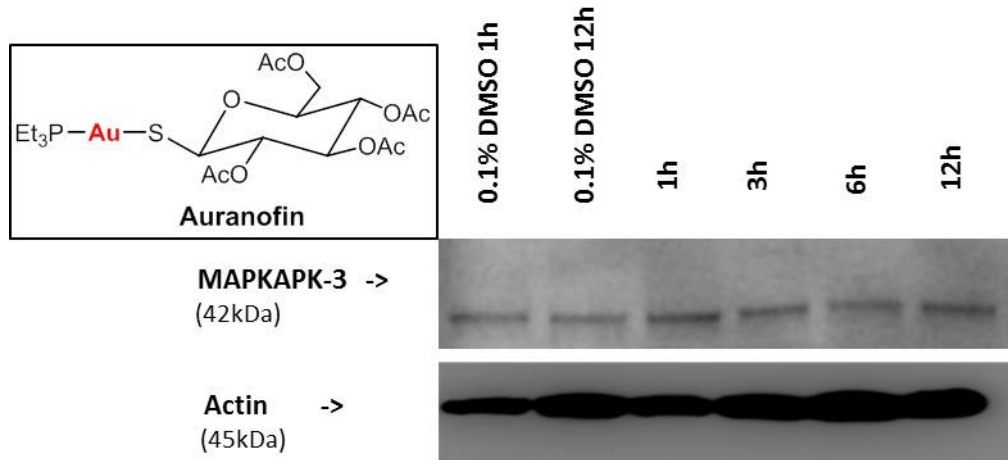


Figure S46. Expression of MAPKAPK-3 in Caki-1 cells in response to Auranofin. Cells were incubated with Auranofin for the indicated times, followed by cell lysis, and Western blot analysis. Blots were probed with anti-β-Actin antibody as a control for protein loading.

14. Effect of compound 3 on Caki-1 mouse xenografts

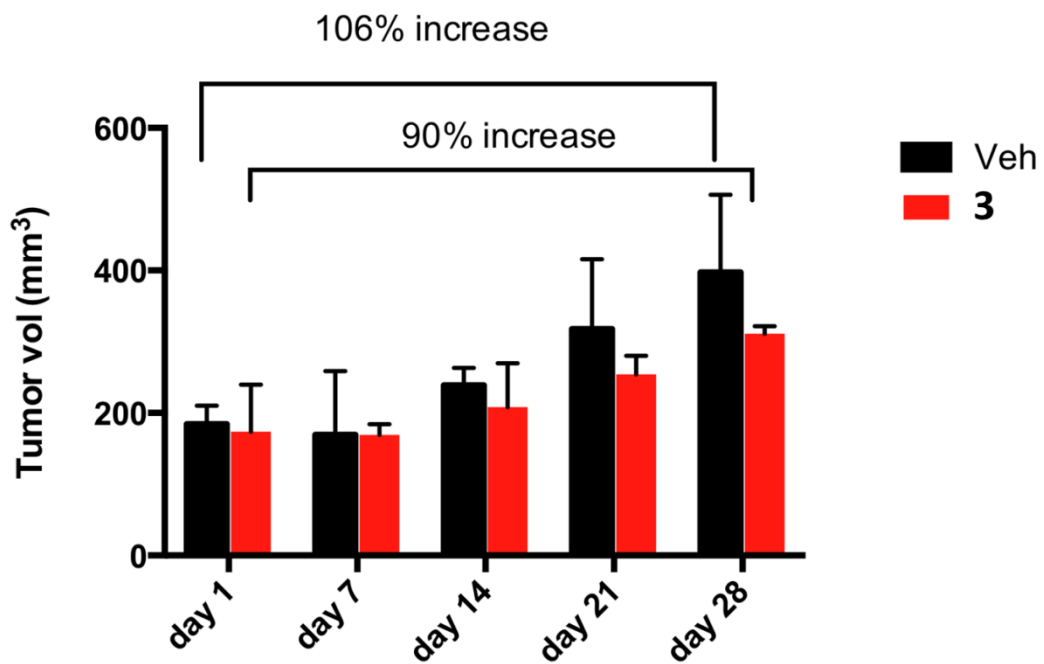


Figure S47. Percent reduction of tumour burden in a cohort of 18 female NOD.CB17-Prkdc scid/J mice inoculated subcutaneously with 8×10^6 Caki-1 cells. The treatment started when tumors were palpable (6 mm diameter). 6 mice were treated with compound 3 (red bars), 6 were treated with the vehicle 100 μl normal saline (0.9% NaCl) (black bars). Compound 3 was administered in the amount of 7.5 mg/kg/every other day.